energies

MDPI

Review

The Role of Fully Coupled Computational Fluid Dynamics for Floating Wind Applications: A Review

Hannah Darling and David P. Schmidt *

Mechanical and Industrial Engineering Department, University of Massachusetts, Amherst, MA 01003, USA
* Correspondence: schmidt@umass.edu

Abstract: Following the operational success of the Hywind Scotland, Kincardine, WindFloat Atlantic, and Hywind Tampen floating wind farms, the floating offshore wind industry is expected to play a critical role in the global clean energy transition. However, there is still significant work needed in optimizing the design and implementation of floating offshore wind turbines (FOWTs) to justify the widespread adoption of this technology and ensure that it is commercially viable compared to other more-established renewable energy technologies. The present review explores the application of fully coupled computational fluid dynamics (CFD) modeling approaches for achieving the cost reductions and design confidence necessary for floating wind to fully establish itself as a reliable and practical renewable energy technology. In particular, using these models to better understand and predict the highly nonlinear and integrated environmental loading on FOWT systems and the resulting dynamic responses prior to full-scale implementation is of increased importance.

Keywords: floating offshore wind; computational fluid dynamics; fully coupled

Citation: Darling, H.; Schmidt, D.P. The Role of Fully Coupled Computational Fluid Dynamics for Floating Wind Applications: A Review. *Energies* **2024**, *17*, 4836. https://doi.org/10.3390/en17194836

Academic Editor: Marcin Wołowicz, Krzysztof Badyda and Piotr Krawczyk

Received: 30 August 2024
Revised: 18 September 2024
Accepted: 23 September 2024
Published: 26 September 2024

1. Introduction

Over the past several decades, the climate crisis has escalated to an unprecedented level of urgency, necessitating immediate and decisive action. According to the Intergovernmental Panel on Climate Change (IPCC), due to disruptive human activities, the planet is facing widespread and sudden changes to the atmosphere, ocean, cryosphere, and biosphere, resulting in significant adverse environmental and humanitarian impacts [1].

Recognizing the urgency of this crisis, the IPCC's Sixth Assessment Report (AR6) has called for substantial reductions in GHG emissions, setting a target of a reduction of at least 43% by 2030 and a 60% reduction by 2035 compared to 2019 levels [1]. A critical step in reaching these goals—while also increasing energy reliability—is to decarbonize and diversify the energy sector by transitioning electricity generation towards renewable energy, which derives from naturally replenishing resources rather than fossil fuels [2,3]. In support of this clean energy transition, the United Nations—in their 28th Conference of the Parties (COP28) annual climate meeting—agreed to triple renewable power generation by 2030, necessitating an additional 7 terawatts (TW) of renewable capacity to be added in the next few years (based on 2023 numbers [4]). Following solar power, the most promising potential clean energy resource is wind, due to its widespread geographic availability, seemingly unlimited reserve, and large pollution-free electricity generation capacity via wind turbines [5–7].

According to the Global Wind Energy Council's 2024 Global Wind Report, the total wind energy installations worldwide (see Figure 1) have surpassed 1 TW in capacity, following the 117 gigawatts (GW) that were added in 2023 alone (a 50% increase from 2022) [8]. Of the current total wind capacity, the majority of installations are onshore, but the space on land is limited with regard to the additional 2 TW capacity required to reach 2030 targets. Therefore, as the technology advances, attention is shifting offshore, where there is more space, fewer obstructions, and a stronger and more consistent wind resource [9–11]. Additionally, offshore

wind turbines can be strategically located near densely populated coastal regions, minimizing transmission losses and providing a reliable power source to areas with high electricity demand [9,12,13].

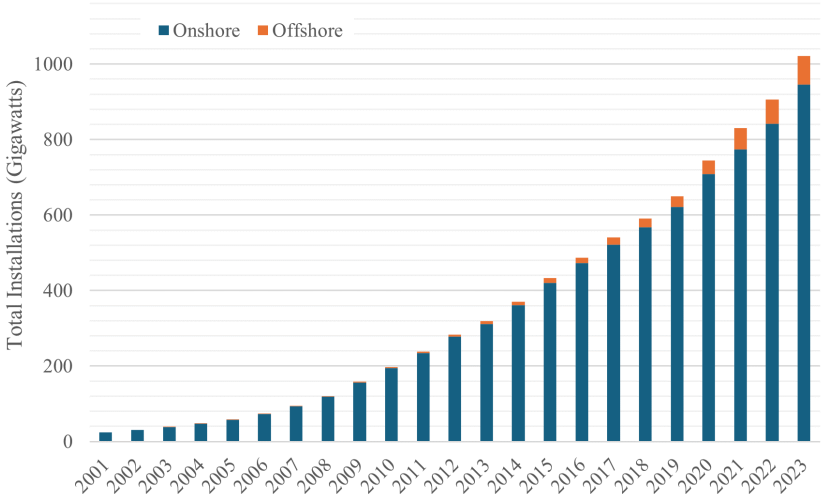

Figure 1. Historic development of total onshore and offshore wind installations (in gigawatts). Data are extracted from the Global Wind Energy Council's 2024 Global Wind Report [8].

The majority of commercial wind turbines are horizontal and three-bladed [10], with the primary distinction between onshore and offshore wind turbines lying in their support structures. Onshore turbines are supported by a simple concrete foundation, while offshore turbine support structures are more complex and expensive and can be either fixed or floating, depending on water depth and seabed conditions [10]. Most operational offshore turbines are mounted on substructures such as monopiles, jackets, tripods, and gravity-base substructures, which are all fixed to the seabed, making them suitable and cost-effective for shallow to intermediate water depths [9,10,14]. However, as water depth increases, the practicality and cost-effectiveness of fixed-support turbines diminishes, making floating offshore wind turbines (FOWTs) a more viable option [15]. For example, in the U.S., waters along the Pacific coast, Gulf of Maine, around Hawaii, and in the Great Lakes are considered too deep (i.e., greater than 60 m) for fixed-bottom systems, so floating substructures would be preferred in these areas [16], as shown in Figure 2.

FOWTs are anchored to the seabed with mooring cables, allowing them to harness wind resources in deeper waters (>60 m), where more than 80% of offshore wind resources are found [10]. This capability is essential for tapping into the abundant wind energy potential and flexible site selection available further from the coast, while also minimizing public concerns for visual, noise, and environmental impacts [9,11,17,18]. These systems provide a solution for deep-water locations, overcoming the limitations associated with fixed-bottom turbines. Consequently, FOWTs are expected to play a critical role in the clean energy transition, significantly contributing to global efforts to mitigate the adverse impacts of climate change, reduce GHG emissions, achieve sustainable energy goals, and foster a resilient and equitable energy future.

While other renewable energy technologies are also crucial players in the above efforts, the present review will focus solely on floating wind energy. Specifically, this paper includes discussions of (1) FOWT technology and industry outlook; (2) the nature of the offshore environment and the dynamic challenges associated with FOWT systems under complex and variable loading; (3) typical FOWT modeling approaches, including their applications and limitations; (4) the role of fully coupled computational fluid dynamics (CFD) modeling approaches for FOWT dynamic analysis and the vast decisions involved in such simulations; and (5) insight into future research directions and opportunities.

Figure 2. Suitability of fixed and floating offshore wind installations along the U.S. coast. Figure is borrowed from the U.S. Department of Energy's Wind Energy Technologies Office [16].

Note that several other reviews have been conducted on modeling techniques for FOWTs (e.g., recent reviews by Subbulakshmi et al. [19], Otter et al. [20], Chen et al. [21], etc.), but few have been conducted specifically on the CFD applications of FOWTs. Recently, Xu et al. [22], Zhang et al. [23] and Haider et al. [24] have conducted reviews on CFD applications in floating offshore wind, including comparisons between uncoupled, partially coupled, and fully coupled analyses. The present review builds on these discussions, but focuses primarily on fully coupled CFD applications in the broader context of FOWT dynamic analysis and considers the vast parameter space and decisions associated with these models. This review also identifies common trends and accuracy–efficiency compromises across recent fully coupled CFD simulations. It also provides a more comprehensive discussion of key research directions, particularly in terms of increasing the accuracy, computational efficiency and adaptability of fully coupled CFD models.

2. Floating Offshore Wind: Overview

The concept of large-scale FOWTs (Figure 3) was first introduced by Professor William E. Heronemus of the University of Massachusetts Amherst in 1972 [25,26]. However, it was not until the mid-1990s (when the commercial wind industry became more established) that the broader research community revisited the concept [27].

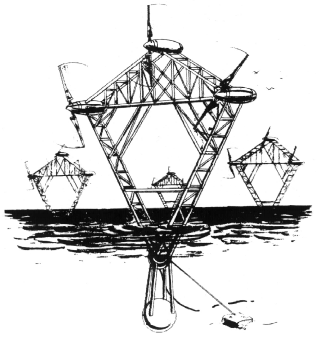

Figure 3. The original concept of floating offshore wind farms, as illustrated in the 1970s by William E. Heronemus of the University of Massachusetts Amherst Wind Energy Center [25,26].

Since then, the floating offshore wind industry has undergone significant growth, drawing inspiration from the marine and offshore oil and gas industries, which have developed advanced technologies for floating structures over the past several decades [9,28]. FOWTs now include various support structure designs, as shown in Figure 4, including spar-type platforms, tension leg platforms (TLPs), semi-submersibles, and barges, each with unique characteristics and advantages depending on the application (see Section 3.3) [10].

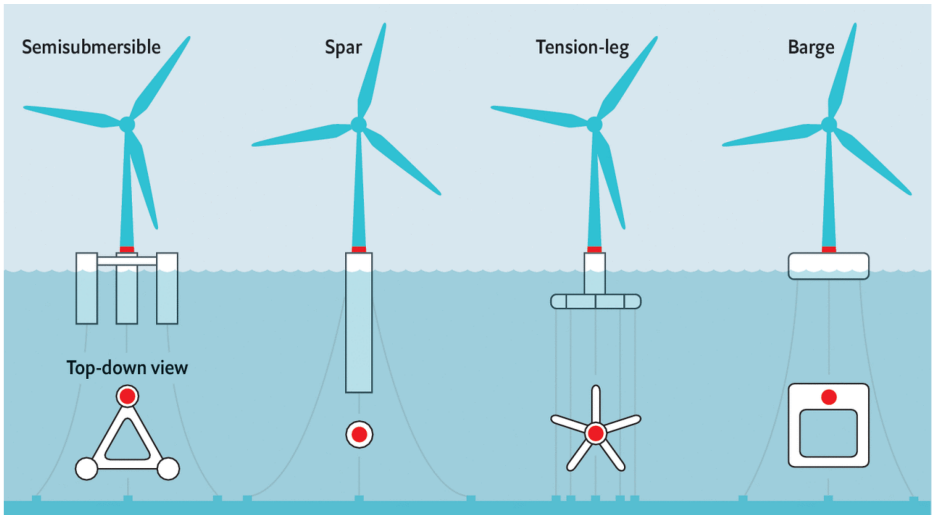

Figure 4. Common floating wind design concepts, including a top-down view with a red dot at the tower-platform connection point. This figure is borrowed from Mei et al. [29].

Several pioneering projects have marked the progress of FOWT technology; Beginning with the deployment of Blue H Technologies' TLP prototype in 2007 [30], and StatoilHydro's Hywind Demo in 2009 [31], there have been several single-turbine floating offshore wind demonstration projects installed around the world [9]. However, the first floating offshore wind farm, Hywind Scotland, was not installed until 2017, comprising five 6 megawatt (MW) turbines on spar-type substructures [32]. Since then, three other floating offshore wind farms have been deployed—WindFloat Atlantic in Portugal (2020) [33], Kincardine in Scotland (2021) [34], and Hywind Tampen in Norway (2023) [35].

By the end of 2023, a total of 236 MW of floating wind capacity had been installed worldwide, and this number is expected to grow substantially in the coming years [8]. Although the current floating wind capacity only contributes to about 0.3% of total offshore wind power, it accounts for 24% of the pipeline for future offshore wind projects. Per the 2023 Offshore Wind Market Report produced by the National Renewable Energy Laboratory (NREL) [36], the global pipeline for floating wind energy was around 102.5 GW (across all stages of development) as of 2022. This capacity increased 69% since the end of 2021, largely attributed to new commercial project announcements, mostly in the United Kingdom. While the majority of the pipeline is currently in the planning stage (see Table 18 in the report by Musial et al. [36]), the outlook of the floating offshore wind industry is promising.

However, at present, FOWTs are not as commercially viable as fixed onshore/offshore wind and other more-established renewable energy technologies. This is largely attributed to their technological immaturity, high capital cost (with the largest contribution from the substructure, i.e., around 40% [9]) and high operation and maintenance (O&M) costs. As a result, there is still significant work to be done to optimize the design and implementation of FOWTs, making them economically competitive compared to other technologies and enabling large-scale commercialization. Specifically, understanding and predicting how these systems behave in a real-world offshore environment is necessary.

3. Dynamic Challenges of FOWTs

Floating offshore wind systems are fairly complex, consisting of a wind turbine, a floating support platform, a control system, and mooring lines anchoring the system to the sea floor. Unlike fixed-bottom onshore or offshore turbines, FOWTs face six degrees of freedom (DOF) of platform motion, meaning they can translate in, and rotate about, all three axes, as shown in Figure 5 [37]. These modes of movement can be excited by the combined influence of marine environmental loads and system restoring loads (see Section 3.3) that act on the turbine and support structure [9,38].

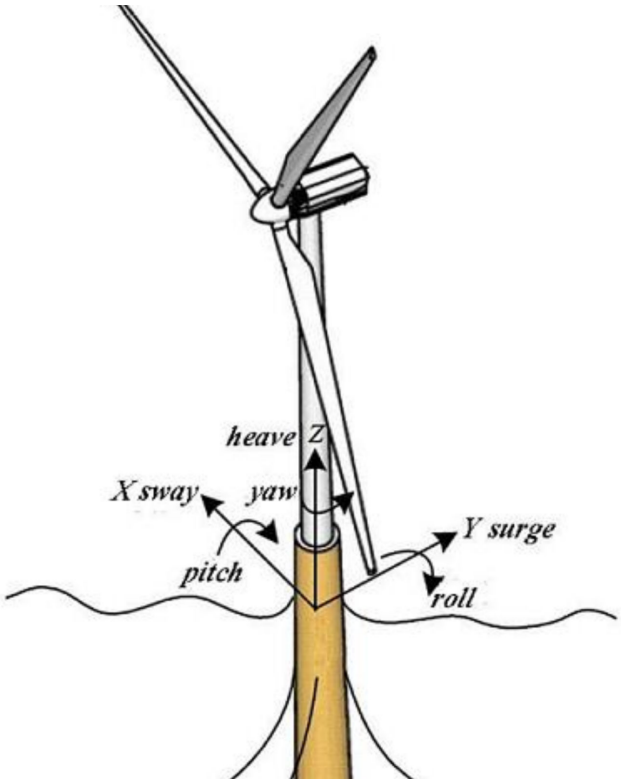

Figure 5. The six-degrees-of-freedom platform motions on a floating offshore wind turbine, borrowed from Hu et al. [37].

FOWTs are exposed to a harsh and complex offshore environment, characterized by a multitude of environmental loading sources (shown in Figure 6), with the largest contributions coming from combined wind and wave effects, which are discussed more in Sections 3.1 and 3.2 [39]. In addition to typical aerodynamic/hydrodynamic loading, FOWTs are subject to several other environmental loads, including seismic activity (e.g., earthquakes and tsunamis) and extreme weather events (e.g., rogue or breaking waves, precipitation, and hurricanes) that can contribute to high-impact and destructive forces [40]. Additionally, marine growth (e.g., barnacles and algae) can add weight and alter the hydrodynamic profile of the structure, thus increasing drag forces [40]. In cold offshore climates, FOWTs can also be subject to additional damage and loading from ice in two forms: (1) ice accumulation on blades and other surfaces from precipitation and sea spray, and (2) collision with sea ice [9,40]. In busy maritime regions, FOWTs are also at risk of ship collisions [9,41].

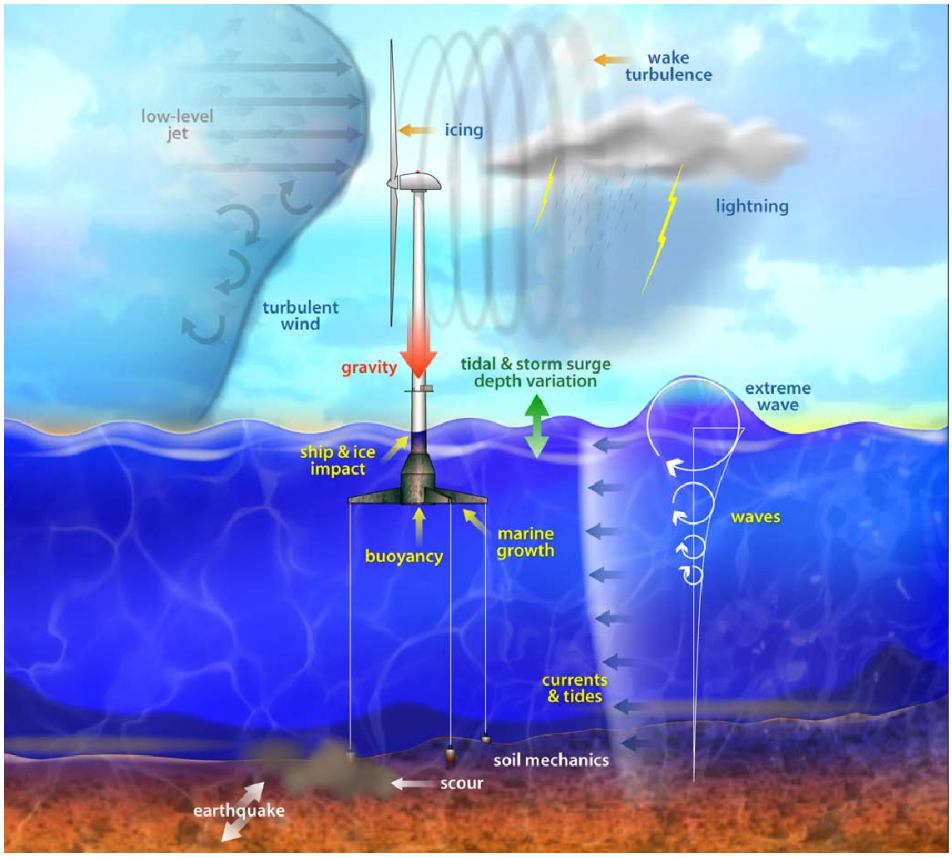

Figure 6. Marine environmental conditions for floating offshore wind, borrowed from Sirinivas et al. [42] (Illustrated by Al Hicks, National Renewable Energy Laboratory).

Offshore environmental loads can vary in magnitude, position, and direction over time, and should be considered in combination due to their simultaneous and interacting dynamic effects on FOWT systems [40,43]. Of particular interest to FOWT designers is the coupled dynamic behavior between turbine aerodynamics and platform hydrodynamics, as discussed in Sections 3.1 and 3.2. FOWT systems are also subject to additional coupled interactions from structural dynamics (e.g., aeroelastic responses due to blade flexibility and hydroelastic responses due to extreme wave loading), mooring line dynamics, and servodynamics (controls) [15], though these aspects are not fully addressed in the present report.

3.1. Aerodynamic Contributions

All wind turbines, onshore and offshore, capture energy from the wind to generate electricity, where more power is extracted with higher wind speeds [44]. However, the wind is also a source of aerodynamic loading that occurs due to wind interactions with the turbine blades and other exposed parts of the structure [39]. These loads are inherently nonlinear and consist of lift forces on the blades that drive energy production when the turbine operates. The loads also include drag forces on all exposed parts of the FOWT system, which dominate when the turbine is parked in high winds [44].

Ocean waves and temperature differences between the sea and air create offshore wind patterns that are distinct from those over land, so our knowledge of wind loads from land-based systems is not entirely transferable offshore [39,40,44]. Additionally, while the wind is generally stronger and more consistent offshore (which is favorable for power production), this wind—like the wind onshore—is still highly irregular and unpredictable due to its inherent spatial and temporal variability [44]: spatial variability includes changes in wind direction and differences in wind speed with height (wind shear); and temporal variability includes long-term changes in mean wind speed from year to year, season

to season, and day to day, as well as short-term fluctuations such as turbulence, gusts, and squalls. This variability results in highly complex and unsteady flow conditions, as listed below, that significantly impact aerodynamic performance of FOWTs [45–47].

- Yawed/skewed inflow: wind flow and rotor are misaligned, i.e., wind encounters rotor off-axis (at an angle) rather than on-axis (perpendicular) [23,48].
- Sheared inflow: wind flow has a vertical wind speed gradient, meaning wind speed varies with height, as mentioned previously [23,49].
- Wake inflow: wind flow of low speed and high turbulence coming from the wake of upwind turbines in a wind farm [23,50].
- Turbulent inflow: wind flow from chaotic and irregular changes in wind velocity and direction [23,51].

These variations lead to fluctuating aerodynamic loading on blade sections, increased peak forces, blade vibrations and considerable material fatigue, and thus can significantly affect the turbine's performance and operational integrity [44]. Additional contributions to the unsteady aerodynamic environment and performance of FOWTs include blade flapping and deflection, dynamic stall, rotational sampling, and tower shadow, which are described more in the literature, e.g., by Manwell et al. [44] and Leishman et al. [45].

A key distinction from fixed turbines is that for FOWTs, these unsteady aerodynamic effects are exacerbated by platform hydrodynamics. The 6-DOF motion of the floating platform excited by incident waves alters the turbine's position/orientation, thus influencing the (already complex) wind inflow conditions faced by the rotor and the overall aerodynamic performance of the FOWT [11,20,23,40]. The motions transmitted from the platform to the turbine contribute to the additional mean rotor tilt angle (which causes significant energy losses), the time-varying geometric angle of attack along the blade sections, the possibility of occurrence of vortex ring state (VRS) conditions, the time-varying rotor induction (dynamic inflow), and an increased occurrence of rotor misalignment (skewed/yawed inflow), and increased blade-vortex interactions, which are all described in detail by Cruz and Atcheson [40].

Of particular interest is the occurrence of VRS conditions, which arise when the rotor is forced into and out of its own wake during platform pitch motions. This phenomenon, depicted in Figure 7, is further discussed in the literature, e.g., by Matha et al. [52], Xu et al. [22], Cruz and Atcheson [40],and Sebastian and Lackner [53]. In addition to wake effects at the individual turbine level, the evolution of the turbine wake and its impact on downwind turbines and farm layout should also be considered [20].

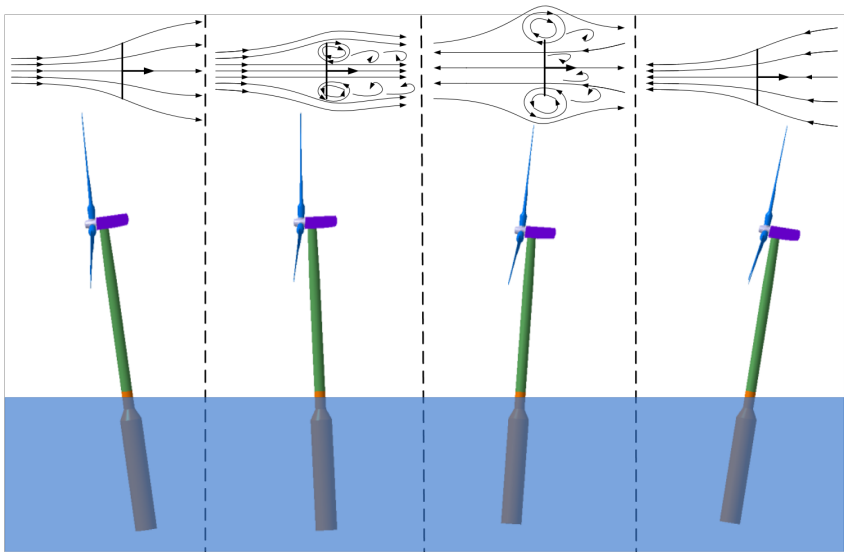

Figure 7. The unsteady effects of platform pitching on the flow field around the rotor, borrowed from Tran et al. [54].

The complicated inflow conditions and unsteady aerodynamic phenomena that FOWTs face are especially difficult to predict and also contribute to the nonlinearity of overall system loading and the dynamic responses of the platform.

3.2. Hydrodynamic Contributions

To add to the complexity of the offshore environment, ocean waves create a dynamic interface for the wind, where surface roughness varies according to wave height and wind shear varies with surface roughness. The interplay between wind and waves is further complicated as wave conditions mainly originate from local and distant winds, and are therefore highly dependent on sea state, which is categorized as either short-term (reflecting typical wind/wave conditions on an average day) or long-term (encompassing extreme events like storms and cyclones) [40]. Resulting wave patterns, shown in Figure 8, include regular waves (mostly sinusoidal, typical of long-distance ocean swell), irregular waves (formed by the interaction of waves from different directions, lacking a defined height or wavelength), and random waves (produced by strong, variable local winds, with unpredictable heights and wavelengths) [55]. Typically, there is also a significant time lag between changes in wind speed and adjustments in wave height/pattern, making the offshore conditions—in particular, load determination—even more complex.

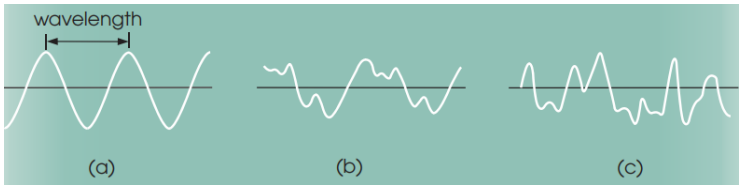

Figure 8. Typical ocean wave patterns: (**a**) regular waves, (**b**) irregular waves, and (**c**) random waves. Borrowed from P.A. Lynn [55].

Hydrodynamic loading on FOWT platforms is generated by a combination of linear drag, radiation, inertia (added mass), incident wave scattering (diffraction), buoyancy (restoring forces), sea currents, and changing water level (from tides), which are further discussed by Barooni et al. [9]. Hydrodynamic loads are highly nonlinear and, as FOWTs increase in size and spread into deeper waters, these effects become more significant, especially under extreme conditions that are occurring with increasing frequency due to climate change [15]. Waves are the main contributor to hydrodynamic loads on FOWTs, inducing cyclic forces that are critical to fatigue loading, especially if they occur near the natural frequencies of towers and support structures [55]. Although they do not typically represent critical loads by themselves, ocean currents are another main hydrodynamic loading source, which can interact with waves and produce combined load effects that require careful consideration in the design and analysis of the FOWT system [39].

Most of the hydrodynamic complexities in FOWT analysis are dominated by fluid–structure interaction (FSI), i.e., the dynamic interplay between the floating platform and the surrounding water. In FSI, the forces from waves and currents drive platform motions, and in turn, the platform's responses influence the surrounding fluid flow, creating a continuous feedback loop between the platform and the water. Some of the complex flow phenomena resulting from this interaction include wave diffraction and radiation, wave run-up and slamming, and vortex shedding [20]. Vortex shedding involves the separation of flow around structural elements, like heave plates, which causes alternating vortices that can induce oscillating forces on the platform, known as vortex-induced vibration (VIV) [56].

In addition to wave-related effects, viscous forces play a crucial role in the hydrodynamic behavior of FOWTs. The viscosity of water affects the drag on the platform and its structural components, leading to energy dissipation and influencing the platform's response to waves. Of particular importance are the viscous drag loads on slender platform components or heave plates that can lead to significant nonlinearities, especially in terms

of wave-frequency and low-frequency platform responses [15]. Viscous forces are also important near the surface of the platform, particularly around sharp corners that are prone to flow separation and vortex shedding [57]. Additional consideration should be given to nonlinear effects from wave breaking, high-steepness waves, and higher-order waves [23].

Simultaneously, the aerodynamic forces on the rotor contribute to the overall system loading and induce rotational moments that influence the platform's dynamic response and further complicate FOWT analysis [11]. For more information on the dynamic complexities of FOWTs, refer to other works, including those by Cruz and Atcheson [40], Matha et al. [52], Xu et al. [22], and Subbulakshmi et al. [19].

3.3. Restoring Systems

In response to the highly coupled and nonlinear loads acting on FOWTs, these systems also face restoring forces that keep the structure upright and prevent overturning. For normal motions, these restoring forces are mainly attributed to (1) hydrostatic effects that are generally assumed to be linear and are dependent on the relative position of the platform's centers of buoyancy and gravity [58], and (2) mooring lines, which are anchored to the seabed and provide nonlinear tension that keeps the platform in position against environmental loading [9]. FOWTs typically use catenary mooring systems, tension-leg (taut) mooring systems, or semi-taut mooring systems—shown in Figure 9—all originating from the oil and gas sector [9,59]. Refer to Rui et al. [60] for an in-depth overview on the different mooring systems used for FOWTs and other floating offshore structures.

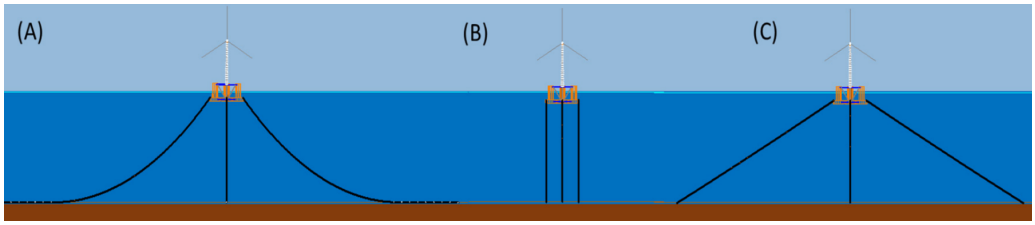

Figure 9. The three types of mooring systems for floating offshore wind turbines: (**A**) catenary, (**B**) taut, and (**C**) semi-taut, borrowed from Barooni et al. [9].

Together, these restoring forces (from hydrostatics and moorings) are essential for maintaining the stability and operational integrity of FOWTs, and also help inform platform design. Floating wind platforms can be categorized into three types based on their stabilization methods under loading: (1) buoyancy-stabilized, (2) ballast-stabilized, and (3) mooring-stabilized. While different FOWT platform concepts tend towards one primary method for obtaining stability, they actually combine aspects of all stabilization methods, as shown in the stability triangle in Figure 10 [27].

Buoyancy-stabilized platforms (e.g., semi-submersible or barge) rely on distributed buoyancy to achieve stability. These platforms tend to have a small draft (depth from water surface), enabling flexible deployment in shallower waters and relatively easy installation and maintenance [30]. However, buoyancy-stabilized platforms (especially semi-submersibles) are relatively complex compared to other platform types, and their large water-plane area results in a large structural mass and higher susceptibility to large wave-induced motions, often requiring more costly design components to mitigate these responses [27].

Ballast-stabilized platforms (e.g., spar buoy) utilize a low center of gravity relative to their center of buoyancy to achieve stability. These platforms offer high inertial resistance to pitch and roll and are relatively easy to fabricate compared to other platform concepts [30]. However, their large draft requirement makes them relatively heavy and expensive, poses significant logistical challenges (e.g., during assembly, transportation, installation, and maintenance), and limits these platforms to deep waters, i.e., over 100 m [30]. Additionally, pitch motions pose a key operational issue for spar buoys, both in terms of their gyroscopic stability and the turbine's performance (due to changing inflow conditions) [58].

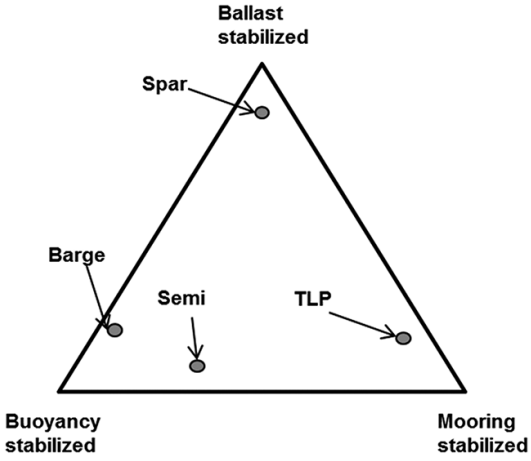

Figure 10. Floating platform stability triangle, with labels of common floating offshore wind platform types, borrowed with permission from Thiagarajan et al. [58].

Finally, mooring-stabilized platforms (e.g., TLP) utilize mooring line tension to achieve stability, and are often considered to be the most stable platform type [27]. These platforms do not require a large water-plane area and tend to have a small draft, enabling a smaller/lighter structure, lower impact on turbine dynamics, and relatively simple assembly and transportation [30]. However, installation is challenging and the dependence on the moorings to prevent overturning leads to high loads on the tendons and anchors, which adds significant operational risk if a cable fails [30].

For more comprehensive discussions on the advantages and limitations of different stabilization methods and their applicability in platform design, refer to other works, including those by Lamei et al. [61], Butterfield et al. [27], Castro-Santos et al. [30] and Thiagarajan et al. [58].

The interaction between restoring forces and environmental loads on FOWTs is a critical player in the complex dynamics of these systems. Therefore, in order to ensure the safe and efficient design and operation of FOWTs, it is important to mitigate and understand the loading that they endure. In particular, the accurate determination of these forces is essential for the dynamic response analysis, design, optimization, control algorithm development, and structural integrity assessment of FOWT systems [9,44].

4. FOWT Modeling

In the floating offshore wind industry, there is an increasing reliance on modeling techniques to predict the loads, dynamic responses, and performance of FOWT systems under various controlled scenarios prior to full-scale implementation [40]. These modeling techniques include both physical (experimental) and numerical approaches, which are used at different stages in the design process [19]. Comprehensive reviews of the various floating offshore wind modeling techniques have been conducted recently by Otter et al. [20] and Subbulakshmi et al. [19].

The scaled physical modeling of FOWTs is crucial for validating numerical models and advancing specific platform concepts toward commercialization [20,40]. However, experimental tests tend to be costly and time-consuming, and additional challenges are present due to the scaling mismatch between the Froude and Reynolds numbers due to working in both air and water, as described by Otter et al. [20]. The present review will not go into any further detail on experimental approaches, but for more discussion, refer to works by Otter et al. [20], Robertson et al. [62], Muller et al. [63], Stewart and Muskulus [64], Gueydon et al. [65], and Cruz and Atcheson [40].

Numerical models, on the other hand, offer the ability to test a broader range of design iterations and environmental conditions at a much lower cost and often shorter time-frame. According to Cruz and Atcheson [40], these numerical models are generally developed either by (1) adapting existing onshore wind turbine design codes by adding modules for

floating platforms and mooring systems, or (2) starting with existing floating platform modeling codes—i.e., those developed for maritime [66] or oil and gas [67] industries—and adding modules for wind turbines, including aerodynamic loading and controls.

These numerical models can be conducted either in the frequency or time domain [40], and can be classified into three levels (low-, mid-, and high-fidelity), where model accuracy and computational cost increase with fidelity, signifying a clear trade-off between accuracy and efficiency in FOWT design [19,20]. FOWT modeling approaches can also be classified as uncoupled (i.e., only considering effects of one environmental condition at a time), partially coupled (i.e., considering effects of multiple environmental conditions—often aerodynamics and hydrodynamics—with one simplified to focus on the other), or fully coupled (i.e., considering combined effects of multiple environmental conditions) [19], which will be discussed more at the end of this section. Similar to fidelity level, more coupling is associated with higher accuracy but also higher computational demands. As a result, models of different levels of fidelity and coupling are often used at different stages of the design process [19,20], as shown in Figure 11.

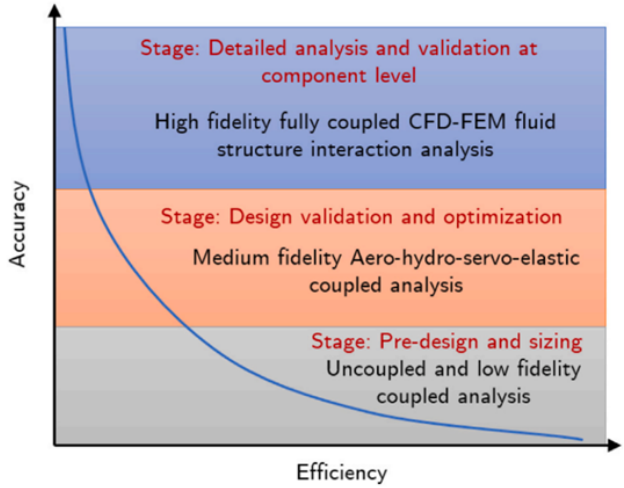

Figure 11. Trade-off between accuracy and efficiency for numerical models at different levels of fidelity, and their application within the floating offshore wind design process. This figure is borrowed from Subbulakshmi et al. [19], which was adapted from Yu et al. [68].

Low-fidelity numerical models are primarily used during the initial FOWT design stages to determine the preliminary sizing and configurations of the system, to simulate linear dynamics, and to reduce the vast design space [19,20]. These models are generally based on static, quasi-static, or steady-state analyses, and include methods such as hydrostatic stability and equilibrium assessments, frequency domain hydrodynamic analysis, empirical methods, and reduced-order state-space models [19]. Some examples of in-house developed codes for low-fidelity modeling in the frequency domain include those by Hegseth and Bachynski [69], Karimi et al. [70], Pegalajar-Jurado et al. [71], and Hall et al. [72].

Mid-fidelity models, also known as engineering-level tools, are typically employed during the design validation and optimization phase for analyzing FOWT loads (both linear and nonlinear) and dynamic behaviors under operational and extreme conditions [19,20]. However, these modeling tools only capture the most significant behaviors of FOWT systems, compromising some accuracy for faster simulation times [19]. The most popular mid-fidelity modeling software packages include OpenFAST [73,74], HAWC2 [75], SIMA [76], Bladed [77], SIMPACK [78], Orcaflex [79], and Flexcom [80].

High-fidelity approaches are often used in the final verification and fine-tuning stages of FOWT design for more detailed investigations [19,20]. These tools include finite element methods (FEM) for structural dynamics and computational fluid dynamics (CFD) for aerodynamics and hydrodynamics [20]. CFD and FEM tools are sometimes coupled together in advanced simulations to analyze interactions of both the fluids and structural

components [19]. In terms of CFD tools, the most common software used for FOWT analysis is OpenFOAM, which is open-source and forked between the OpenFOAM Foundation [81] and OpenCFD Limited [82]. Some of the most popular commercial CFD codes are Siemens Simcenter's StarCCM+ [83] and Ansys Fluent [84]. A few other CFD codes for FOWT applications include the commercial codes CONVERGE CFD [85] and Helicopter Multi-Block Code (HMB) [86], and in-house codes like ReFRESCO [87] and CFDShip-Iowa [88].

High-fidelity models implement the basic governing equations with minimal simplifications [19], therefore making them highly accurate and predictive compared to lower-fidelity numerical modeling approaches. For example, when analyzing the hydrodynamics of FOWT platforms, mid-fidelity methods like Morison's equation (ME) and the potential flow (PF) theory [89] are commonly used but are limited in their ability to capture (1) critical physical mechanisms such as fluid viscosity, wave diffraction and radiation, (2) nonlinear interactions like wave climbing and wave slamming, and (3) complex flow patterns like vortex shedding (especially around heave plates), which are all vital for an accurate analysis of FOWT systems [20,22,52]. CFD offers a more sophisticated alternative that can model these intricate flow mechanisms and capture free surface effects with greater accuracy, providing a more detailed and reliable understanding of the hydrodynamic loads and motion responses of FOWT platforms, especially in scenarios involving complex geometries and nonlinear wave-structure interactions [20,22]. Similarly, in the aerodynamic analysis of FOWTs, traditional mid-fidelity approaches like blade element momentum (BEM) theory [90] cannot accurately represent complex aerodynamic behaviors (e.g., unsteady aerodynamic effects and blade–wake interactions [53]). This limitation occurs because the reality of the offshore environment (see Section 3.1) differs greatly from the ideal steady and on-axis wind inflow assumptions of BEM. Therefore, high-fidelity CFD tools are necessary to effectively capture these effects as well.

While all modeling approaches play a unique and important role in FOWT design, the remainder of this review will focus solely on high-fidelity numerical modeling, in particular CFD approaches. For more information on low- and medium-fidelity numerical modeling approaches for FOWTs, refer to the literature (e.g., recent reviews by Subbulakshmi et al. [19], Fadaei et al. [91] and Otter et al. [20], and other works by Cordle et al. [92], and Cruz and Atcheson [40]).

FOWT modeling approaches can also be classified as uncoupled, partially coupled or fully coupled, as discussed in detail in the review by Subbulakshmi et al. [19]. Uncoupled (or component-level) studies on FOWTs only consider the effects of one environmental loading condition (i.e., either wind or waves) at a time. For instance, uncoupled hydrodynamic studies on FOWTs only consider the effects of waves on the floating platform and neglect the wind acting on the turbine. Meanwhile, uncoupled aerodynamic studies neglect the wave loads and 6-DOFs of the floating platform, essentially treating the system as a fixed, land-based case only under the influence of wind loading [19]. Since this approach greatly simplifies analysis by isolating the effects of each environmental factor, uncoupled studies are abundant in the literature.

Partially coupled (or system-level) studies on FOWTs consider both aerodynamic and hydrodynamic loads, but with one aspect simplified to focus on the other. For example, when studying the aerodynamics of the turbine, prescribed platform motions are typically used to simplify the hydrodynamics [19,22]. This approach is often used in FOWT research to investigate the effect of individual platform motions (with most attention given to surge and pitch) on the unsteady aerodynamic performance of the turbine. When studying the hydrodynamics of the floating platform, aerodynamic forces on the turbine are approximated [19,22]. Partially coupled analysis is typically used in initial design stages of FOWTs for understanding the underlying mechanisms of aero/hydro dynamic interaction and performance [22].

Examples of uncoupled and partially coupled CFD studies are summarized and reviewed by Xu et al. [22], Zhang et al. [23], and Haider et al. [24]. In general, uncoupled and partially coupled studies are relatively simple, computationally efficient, and valuable

in preliminary design stages, but they do not accurately represent real turbine–platform interactions. This limitation has shifted research efforts towards fully coupled CFD to simulate FOWTs under more realistic conditions [19]. A fully coupled analysis takes into account the combined influence of multiple dynamic effects. At present, the majority of fully coupled CFD studies on FOWTs focus on aero–hydro dynamic coupling, but research interests are expanding to incorporate additional aspects of these highly integrated systems, notably mooring dynamics, structural dynamics, and servodynamics. Although fully coupled CFD simulations are more complex and computationally demanding, they are crucial for accurately simulating the interactions between the FOWT and the varying loading sources it is subject to, enabling a more comprehensive and holistic understanding of these systems.

The next section of this review builds on discussions by Xu et al. [22], Zhang et al. [23], Subbulakshmi et al. [19], Amiri et al. [93] and other key studies in the field to explore the role of fully coupled CFD in predicting FOWT system responses. Specifically, this section identifies some notable fully coupled CFD studies (particularly, fully coupled aero-hydro studies) and the key numerical methods associated with this type of modeling.

5. Fully Coupled CFD Approaches

As discussed in previous sections, fully coupled CFD plays a critical role in the design and analysis of FOWTs. Since these simulations are computationally expensive compared to lower-fidelity modeling approaches, it is necessary for the research community to be intentional about the simulations that are conducted.

As a result, FOWT researchers have established multiple representative prototypes, including comprehensive experimental data, to aid in the advancement of CFD modeling approaches [23]. These references provide detailed design parameters and simulation blueprints for CFD researchers to follow, and establish a benchmark for validating CFD results against experimental measurements. Some key prototypes include those for specific platforms or turbines, and serve as a basis for many CFD studies. These prototypes are discussed in detail by Zhang et al. [23], but are summarized here: Representative prototypes for floating platforms include the OC3 Hywind [94], COREWIND WindCrete [95–97], OC4 DeepCWind [98,99], OC5 DeepCWind [100,101], OC6 Phase I-III DeepCWind [102,103], OC6 Phase IV Stiesdal TetraSpar [103,104], VolturnUS-S [105], COREWIND Activefloat [95,97], 5 TLP Baseline designs [106], and ITI Barge [107,108]; representative prototypes for the wind turbines used in FOWT systems include the NREL 5MW [109], DTU 10MW [110], IEA 15MW [111], and IEA 22MW [112].

Currently, the majority of fully coupled CFD studies focus on aero–hydro coupling, as this is the most significant interaction in FOWT analysis and can be addressed solely within CFD. Many of these studies are summarized in Table 1.

Table 1. Summary of some recent CFD studies on the fully coupled aero–hydro dynamic analysis of FOWTs.

Author/Ref.	Year	Software	Ref. Turbine	Ref. Platform
Ren et al. [113]	2014	Ansys Fluent	NREL 5 MW	TLP
Quallen & Xing [114]	2016	CFDShip-Iowa	NREL 5 MW	OC3 Hywind Spar
Tran & Kim [115]	2016	STAR-CCM+	NREL 5 MW	OC4 DeepCWind
Leble & Barakos [116]	2016	HMB2	DTU 10 MW	WindFloat
Li et al. [117]	2016	OpenFOAM	NREL 5 MW	OC4 DeepCWind
Liu et al. [11]	2017	OpenFOAM	NREL 5 MW	OC4 DeepCWind
Tran & Kim [118]	2018	STAR-CCM+	NREL 5 MW	OC4 DeepCWind
Ren et al. [113]	2014	Ansys Fluent	NREL 5 MW	TLP

Table 1. *Cont.*

Author/Ref.	Year	Software	Ref. Turbine	Ref. Platform
Zhang & Kim [119]	2018	STAR-CCM+	NREL 5 MW	OC4 DeepCWind
Zhou et al. [120]	2019	OpenFOAM	NREL 5 MW	OC4 DeepCWind
Huang et al. [121,122]	2019	OpenFOAM	NREL 5 MW	OC3 Hywind Spar
Cheng et al. [123]	2019	OpenFOAM	NREL 5 MW	OC4 DeepCWind
Zhou et al. [124]	2021	OpenFOAM	NREL 5 MW	OC4 DeepCWind
Zheng et al. [125]	2021	OpenFOAM	NREL 5 MW	OC3 Hywind Spar
Zhou et al. [51]	2022	OpenFOAM	NREL 5 MW	OC4 DeepCWind
Xie & Sadique [126]	2022	CONVERGE	NREL 5 MW	OC4 DeepCWind
Huang et al. [127]	2023	OpenFOAM	NREL 5 MW (×2)	OC3 Hywind Spar
Huang et al. [128]	2023	OpenFOAM	NREL 5 MW	Bionic Fractal Semi-Sub
Yu et al. [129,130]	2023	OpenFOAM	NREL 5 MW	OC4 DeepCWind
Feng et al. [131]	2023	STAR-CCM+	NREL 5 MW	OC4 DeepCWind
Alkhabbaz et al. [132]	2024	STAR-CCM+	NREL 5 MW	OC4 DeepCWind
Sadique et al. [133]	2024	CONVERGE	Siemens 3.6 MW	OC6 Stiesdal TetraSpar

Of these coupled aero–hydro dynamic studies, most are conducted using the open-source OpenFOAM CFD software directly (e.g., studies by Yu et al. [129,130], and studies by Zhou et al. [51,120,124]) or in a tool that is developed based on OpenFOAM, i.e., naoe-FOAM-SJTU (e.g., studies by Li et al. [117], Huang et al. [121,122,128], Cheng et al. [123], Zheng et al. [125], and Liu et al. [11]).

The second most popular CFD software for fully coupled CFD analyses is STAR-CCM+ (e.g., see studies by Tran and Kim [115,118], Zhang and Kim [119], Feng et al [131], Huang et al. [127], and Alkhabbaz et al. [132]). Some other fully coupled studies are conducted in other CFD tools including Ansys Fluent [113], CONVERGE [126,133], HMB2 [116], and CFDShip-Iowa [114], for example.

All of the studies listed in Table 1 use the NREL 5 MW reference turbine in their simulations, with the exception of Sadique et al. [133], who reference the 3.6 MW Siemens Gamesa wind turbine for OC6 Phase IV, and Leble and Barakos [116], who reference the DTU 10 MW turbince. For the floating platform, most of the listed studies use either the OC3 Hywind spar buoy or the OC4 DeepCWind semi-submersible platform, with the exception of Sadique et al. [133], who reference the OC6 Phase IV Stiesdal TetraSpar platform, Leble and Barakos [116], who reference the WindFloat, Ren et al. [113], who use a TLP, and Huang et al. [127], who use a novel bionic fractal semi-submersible.

In order to further advance towards more realistic simulations, there is also an increasing interest in introducing structural models into the current framework through CFD-FEM coupling to account for the flexible components of FOWT systems and understand their responses under loading. Although both wind and waves affect the elastic behavior of FOWTs, most CFD-FEM to date only focus on aeroelastic effects on turbine blades (e.g., [134–136]), often treating the floating platform as a rigid body [23]. However, as modern FOWTs increase in size, the influence of flexibility of both the blades and platform will become significantly more relevant and thus need to be incorporated into the design [23]. These trends introduce more intricate flow interactions and necessitate integrated approaches in hydroelasticity, aeroelasticity, and structural dynamics. Therefore, some efforts should shift to the aero–hydro–elastic performance of FOWTs, particularly for the situations of large-scale blades and extreme weather conditions.

Currently, CFD studies that encompass the full spectrum of aero–hydro–elastic behaviors remains scarce due to the high computational requirements of these advanced simulations, so significant future research and development will be necessary in this area [23,93].

5.1. Computational Methods

In order to describe the motion of viscous fluids (e.g., air and water), fluid dynamicists utilize a set of partial differential equations (PDEs) that combine conservation of mass and momentum with body forces, pressure forces, and viscous forces [137]. These PDEs are known as the Navier–Stokes (NS) equations and for most cases, they cannot be solved analytically [137]. Instead, numerical approaches, i.e., CFD, are necessary to obtain an approximate solution to the NS equations; in CFD, this involves the evaluation of flow variables (e.g., pressure and velocity) at every point in a discretized computational domain [19,137].

The present review provides an overview of the CFD modeling process for FOWT applications largely influenced by discussions by Shourangiz-Haghighi et al. [5] and Zhang et al. [23]. After identifying the problem to be solved—which involves the clear definition of goals and the problem domain (i.e., whether focused on hydrodynamics, aerodynamics, or both)—the main steps in CFD modeling include (1) pre-processing, (2) solving, and (3) post-processing.

Pre-processing involves necessary case setup, including geometry construction, mesh generation, physics definition, and solver settings, as defined by Shourangiz-Haghighi et al. [5]. In the solving stage, computers are used to carry out the simulation, using specified numerical methods to discretize the NS equations and solve the resulting systems of equations at each point in the domain [23,137]. Once calculations are complete, the numerical results are examined and analyzed in the post-processing stage [5,23]. Since the pre-processing stage is where the majority of the critical decisions are made that influence the accuracy and efficiency of CFD models, the key components of this stage are further discussed in the remainder of this section.

5.1.1. Geometry and Mesh Construction

The first step in pre-processing is constructing a digitized model, typically using computer aided design (CAD) tools, that accurately describes the geometry of the entire FOWT system, with specific attention to the blades and other complex structural components [5,23].

Another crucial step is generating the mesh, which is a discrete representation of the geometric domain that divides the solution space into finite subdomains, such as elements or control volumes, at which flow variables are calculated [137]. Note that mesh resolution (i.e., how spaced out the cells are in a computational domain) has a significant impact on the accuracy and computational cost of CFD simulations. In most cases, a finer mesh leads to higher accuracy, which is critical for predicting the critical flow phenomena associated with FOWT systems. However, increasing mesh density also leads to an exponential increase in computational demand, which represents the first of many trade-offs between accuracy and efficiency in CFD modeling.

Types of mesh for wind turbine applications generally include (1) structured mesh, which is the simplest structure—offering high resolution, easy convergence, and low memory usage (according to the review by Shourangiz-Haghighi et al. [5])—but is sub-optimal for complex geometries like highly twisted blades, (2) unstructured mesh, which is the most flexible structure for complex geometries but has higher computational requirements, and (3) hybrid mesh, which is widely used in wind turbine modeling as it combines the benefits of structured and unstructured mesh, employing structured mesh around important regions (e.g., the boundary layers of blades) and unstructured mesh in the remainder of the domain [5].

It is also important to consider how to treat the mesh if the body is moving in the presence of a free surface (i.e., the air–water interface) [23]. The main approaches include dynamic mesh techniques—such as remeshing, sliding mesh [113,127] (also known as arbitrary mesh interface (AMI) in OpenFOAM [11,138]), and deforming mesh [121]—and overset mesh techniques [114,115,118,119,132], each with their own advantages and limitations. For example, in terms of hydrodynamic modeling of FOWTs, dynamic mesh

techniques may face reduced accuracy and numerical stability due to poor mesh quality in scenarios involving significant platform motion, whereas the overset mesh technique maintains mesh quality even with substantial motion but requires extensive expertise in mesh generation and higher computational costs [22]. In their fully coupled analysis of a novel semi-submersible FOWT under wind–wave excitation conditions, Huang et al [127] utilized both dynamic and overset mesh techniques: overset mesh is used for the 6DOF platform motion region, and the blade rotation region is realized via sliding mesh with superimposed motion.

5.1.2. Physics Definition

Also related to the complexities of interface treatment is how the free-surface is represented, either by interface tracking or interface capturing [93,139,140], as shown in Figure 12.

Interface tracking (Figure 12a) utilizes a moving (Lagrangian) grid that conforms to the free surface to follow its position over time, essentially treating it as a boundary [93,137]. While this method is accurate for smooth and well-defined interfaces, larger deformations (e.g., from ocean waves) require remeshing techniques that are computationally demanding and prone to numerical errors [93]. Therefore, the interface capturing method (Figure 12b) is more commonly used in FOWT analysis, utilizing a fixed (Eulerian) grid covering the fluids on both sides of the interface and capturing the shape of the surface via algorithms such as volume of fluid (VOF) and level set method (LSM) [93,137]. LSMs represent the surface as the zero contour of a higher-dimensional level set function [114], while VOF calculates the fraction of fluid within each computational cell. To date, most of the fully coupled CFD simulations on FOWT aero/hydro dynamics utilize VOF (e.g., see [11,113,115,119,121,122,127,132]).

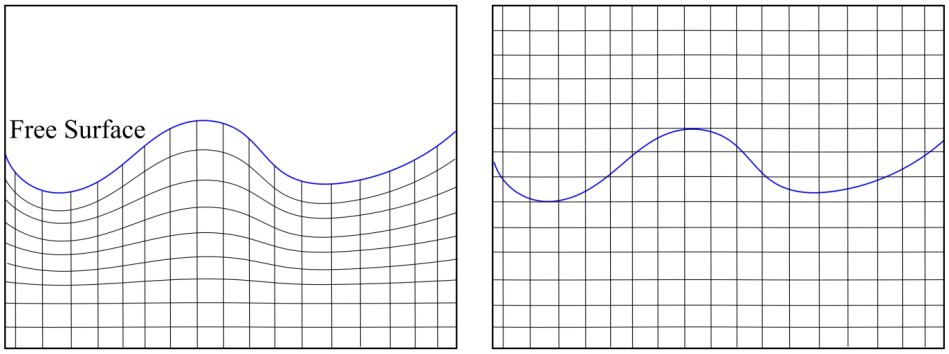

Figure 12. The two main approaches for free surface modeling in CFD: (**a**) interface-tracking and (**b**) interface-capturing. Borrowed from Amiri et al. [93].

In the VOF method [141], the free surface is represented by the volume fraction, α, as illustrated in Figure 13. For two-phase air–water flow, the volume fraction is distributed based on the fluid that occupies each near-interface cell: where $\alpha = 1$ is for water, $\alpha = 0$ is for air, and the free surface is where $0 < \alpha < 1$.

The respective volume fractions of air and water in each cell of the mesh are then used as weighting factors to determine the properties (i.e., density, ρ, and viscosity, μ) of the mixture occupying that cell:

$$\rho_{cell} = \alpha\, \rho_{water} + (1 - \alpha)\, \rho_{air} \quad (1)$$

$$\mu_{cell} = \alpha\, \mu_{water} + (1 - \alpha)\, \mu_{air} \quad (2)$$

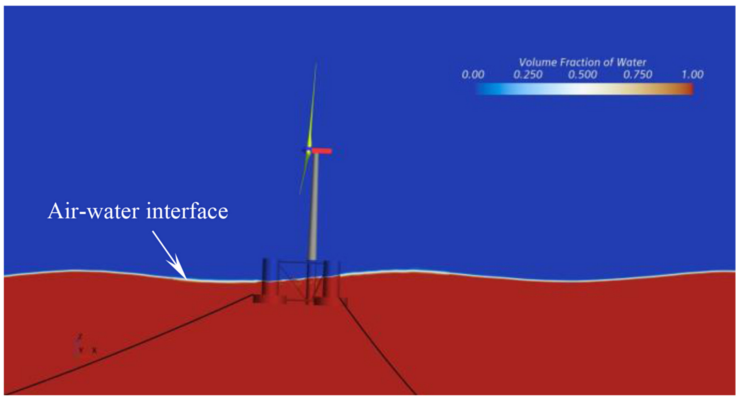

Figure 13. An example of how the volume fraction, α, is used in volume of fluid methods for capturing the air-water interface, where $\alpha = 1$ is water (colored in red), $\alpha = 0$ is air (colored in blue) and the range in between marks the free surface. This figure is borrowed from Alkhabbaz et al. [132].

In order to simulate the 6-DOF motions of the FOWT platform, these fully coupled CFD models must also incorporate some sort of FSI model. FSI modeling methods are categorized as being either monolithic or partitioned [142]. The monolithic approach in FSI modeling solves the coupled fluid and structural dynamics simultaneously within a unified framework, treating interfacial conditions implicitly. While potentially more accurate, this method requires significant computational resources and expertise to develop, as it requires solving large nonlinear systems of equations. Conversely, the partitioned approach solves the fluid and structure dynamics separately, using distinct computational fields and explicitly exchanging information at the interface. This method tends to be more flexible, allowing for the integration of existing solvers and reducing code development time, so it is preferred for floating offshore wind applications [142].

For example, many of the fully coupled aero–hydro studies based on STAR-CCM+ use a partitioned approach known as the dynamic fluid body interaction (DFBI) method to simulate the 6-DOF rigid body motion of the platform (e.g., see studies by Tran and Kim [115], Zhang and Kim [119], Feng et al [131], Huang et al. [127], and Alkhabbaz et al. [132]). In the DFBI method, the governing equations of motion are solved by calculating the resultant force and moment on the body due to the surrounding fluid flow. This information is then used to update the body's position over time [127]. It is important to note that currently, most FOWT modeling approaches assume the rigidity of the floating platform. However, as floating turbines (and thus, their platforms) get larger and relatively more slender, this rigid-body assumption may lead to the overestimation of fluid forces. Therefore, future research may require the inclusion of hydro-elasticity effects [93].

Establishing suitable boundary conditions is also necessary to describe the surface treatment of the individual FOWT components and the extent of the computational domain. Of particular interest is the inlet boundary condition, at which the desired inflow conditions are established, typically based on specified wind velocity profiles (e.g., logarithmic or power–law distribution to simulate wind shear [44]) or wave theories (e.g., linear/Airy wave theory or nonlinear wave theories like Stokes, Cnoidal or Solitary wave theory [57]).

Note that the majority of fully coupled studies are limited to regular wave conditions in simulations due to the high computational demands of more realistic irregular wave conditions over an extended duration (which is required to capture nonlinearities) [93]. Exploring another alternative, Zhou et al. [124] assess the applicability of focused waves, particularly reconstructed focus waves, for capturing nonlinear effects with lower simulation times. Note that focused waves [143] comprise a modulation of a series of regular wave trains generated from a prescribed wave spectrum and superimposing crests, while the reconstructed focus wave defined in this study is built up based on the largest wave generated in an irregular wave simulation. From this study, it was found that the FOWT hydrodynamic characteristics using unstructured focused waves are very similar to those obtained with irregular waves, as shown in Figure 14, thus determining that this wave type

can be a good alternative for extreme wave studies. For more information on how these waves were constructed and all associated analysis, refer to Zhou et al. [124].

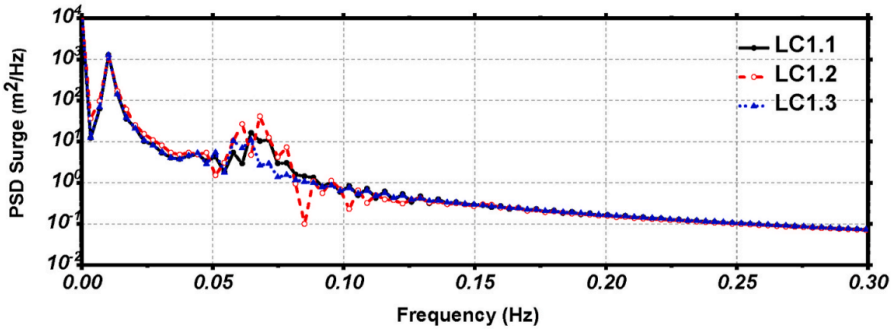

Figure 14. Example results borrowed from the fully coupled aero-hydro dynamic CFD study by Zhou et al. [124]. This figure shows the power spectral density (PSD) of the platform surge response under three different wave conditions: focused waves (LC1.1), irregular waves (LC1.2), and reconstructed waves (LC1.3).

As identified by Zhang et al. [23], many CFD studies of FOWTs are conducted in numerical wave tanks (NWTs), which require specific boundary conditions to model wave generation and propagation. Typical wave generation methods include relaxation zone, static boundary, dynamic boundary, mass source, and impulse source; and typical wave propagation methods include relaxation zone, static boundary, dynamic boundary, numerical beach, geometrically sloped beaches, and cell stretching. Refer to the work by Windt et al. [144,145] for more information on these wave generation/propagation methods and their typical application. Once the waves are established in the computational domain, methods must also be employed to avoid wave reflection at the domain boundaries [93]. According to Amiri et al. [93], typical approaches to dampen the waves include: (1) utilizing a coarser grid resolution near the boundary, and (2) establishing damping/relaxation zones near the boundaries in which specific functions are used to force the waves towards the undisturbed free surface.

For example, the studies by Zhou et al. [51,120,124] use the built-inwaves2Foam toolbox [146] in OpenFOAM for free surface wave generation and absorption in a NWT. They also utilize relaxation zones near the inlet (for better wave quality) and outlet boundaries (to avoid reflection). Most of the other fully coupled aero–hydro dynamic studies from Table 1 also include damping/relaxation zones to prevent numerical wave reflection back into the domain (e.g., [11,113,115,119,125,128,132]).

Addressing turbulent flow is another important aspect in FOWT modeling due to the complexities associated with free-surface waves [15] and the varying size and frequency of eddies in the rotor wake [19]. Typical turbulence models include direct numerical simulation (DNS), large eddy simulation (LES), (Unsteady) Reynolds-averaged Navier–Stokes ((U)RANS) equations, and detached eddy simulation (DES).

DNS models directly solve the full NS equations on an extremely fine computational grid, capturing all relevant turbulence scales, including the smallest eddies [52,93]. While this approach is highly accurate, the large mesh requirements make it too expensive and thus impractical for complex geometries and high Reynolds numbers associated with FOWT environments [19]. LES approaches are similar to DNS, but rather than directly solving for all turbulent length scales, LES approaches apply a spatial filter to directly resolve larger turbulence structures and employ sub-grid scale (SGS) models for the smaller eddies [52,137]. LES is highly accurate and well-suited for simulating turbulent wakes, but it requires significant computational resources, particularly when applied near the boundary layer of turbine blades [23,52].

Rather than directly solving the turbulence, RANS/URANS approaches model turbulent flow by decomposing the NS equations into their time-averaged and fluctuating flow components via Reynolds decomposition [19,40,147]. Note that URANS extends RANS

to capture unsteady effects, i.e., URANS averages overensembles, or sets of statistically identical realizations, rather than over the entire time, in order to remove random eddies [137]. The resulting nonlinear Reynolds stress term from the Reynolds decomposition requires additional sub-models—including eddy-viscosity models (EVMs) or Reynolds stress models (RSMs) [148]—to close the (U)RANS equations [93]. The most commonly used and well-known sub-models are EVMs, particularly two-equation relations, including k-ϵ, k-ω, and k-τ, which are defined in great detail by J. Bredberg [148]. As identified by Amiri et al. [93], (U)RANS is the most widely used turbulence model in FOWT simulations, typically combined with two-equation models such as k-ϵ, k-ω, and k-ω shear stress transport (SST) for hydrodynamic analysis, and k-ω and k-ω SST for aerodynamic analysis [93].

The most common turbulence model used in fully coupled aero–hydro dynamic simulations is the RANS/URANS based k-ω SST model, which utilizes k-ω for the inner region of a surface boundary layer and k-ϵ for the far-field, free shear flow. This method is also known as Menter's Shear Stress Transport, as outlined by F.R. Menter [149]. For the full expression of this model, refer to the original source (i.e., Menter [149]), or to the studies by Zhang and Kim [119] or Zhou et al [120], as both use the k-ω SST turbulence model and provide a good overview of what this method entails. Some other fully coupled CFD studies that use this model include those by Huang et al. [121,122,127], Cheng et al. [123], Tran and Kim [115], Liu et al. [11], and others by Zhou et al. [51,124].

Another option for modeling the turbulence for FOWT applications is DES, which is a hybrid approach, utilizing (U)RANS to model the small-scale turbulence in near-wall regions (e.g., around turbine blades), and LES for the rest of the flow field [19,52,93]. Typically, a length scale function is pre-defined to trigger the switch between U(RANS) and LES [19]. DES is an effective way to reduce the computational demands of full LES modeling while still capturing critical aspects of the flow field, especially wake dynamics. For example, Quallen and Xing [114] use a hybrid delayed DES (DDES) approach to predict unsteady separated flows. This DDES method employs LES in regions of relatively large turbulent length scale, and and a URANS k-ω SST model for remaining regions with smaller turbulent length scales.

Another key decision in FOWT modeling is how to model the physical rotor; either using (1) actuator models, which represent the blades by body force, or (2) direct models, which represent the blades by computational and refined blade-resolved mesh [22]. Actuator models can be categorized as actuator disk models (ADM), actuator line models (ALM), or actuator surface models (ASM), as shown in Figure 15. For more details on the specifics of each, refer to Xu et al. [22] or Sanderse et al. [150].

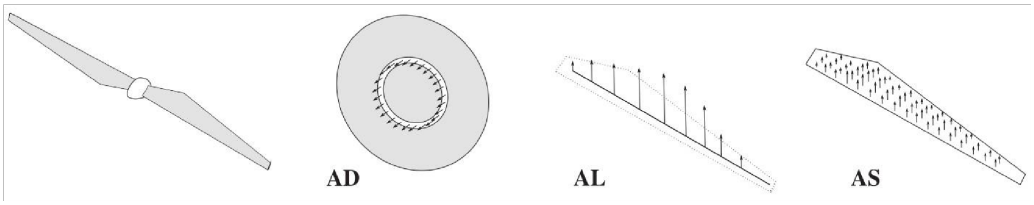

Figure 15. The image on the far left shows a two-bladed turbine rotor. To the right are three actuator concepts used in the computational fluid dynamics modeling of wind turbines: actuator disk (AD), actuator line (AL) and actuator surface (AS). This figure is borrowed from Sanderse et al. [150].

Actuator models are relatively simple and computationally inexpensive, as they do not model the rotor geometry, thus reducing mesh requirements [19,22]. However, since these models avoid solving the surface boundary layer of the blades, they are highly dependent on existing airfoil data, which limits their applicability for novel blade design [22]. In contrast, direct blade-resolved modeling, though computationally intensive, is more precise and suitable for all applications as it provides detailed flow fields on the surface of the blades [22]. As a result, both approaches are widely used in fully coupled FOWT analysis:

actuator models (especially ALM) for their simplicity and efficiency in many scenarios, and direct blade-resolved models for their accuracy and detailed analysis capabilities.

Notably, Cheng et al. [123] develop a fully coupled aero–hydro dynamic model for FOWTs in OpenFOAM, called FOWT-UALM-SJTU. This solver combines an unsteady actuator line model (UALM) for turbine aerodynamics and the two-phase CFD solver naoe-FOAM-SJTU for platform hydrodynamics. Since then, other researchers have also used this tool to investigate the aero–hydro coupling of FOWTs (e.g., Huang et al. [121,122,128], Cheng et al. [123], and Zheng et al. [125]).

Meanwhile, some studies that utilize blade-resolved modeling approaches for the turbine rotor include those by Quallen and Xing [114], Ren et al. [113], Liu et al. [11], Zhou et al. [120,124], Tran and Kim [115,118], Zhang and Kim [119], and Feng et al. [131], for example. These blade-resolved calculations are extremely expensive. The work of de Oliveira et al. [151] examines the cost of these high-fidelity simulations and offers recommendations for solver settings.

Aeroelasticity is another important factor in wind turbine design and is discussed further in Xu et al. [22], requiring both aerodynamic models in CFD to determine the forces exerted on turbine blades and structural models (e.g., 3D FEM and 1D equilibrium beam model (EBM)) to determine the structure dynamics [22]. For example, Yu et al. [134] introduce a new elastic actuator line model (EALM) integrated within OpenFOAM to analyze the aeroelastic performance of the NREL 5 MW wind turbine, focusing on blade deformation effects. The study demonstrates that blade elasticity amplifies tower shadow effects, leading to decreased and unstable power and thrust, especially in the wake of upstream turbines, which is critical for offshore wind farm applications.

Additional consideration should be given to the mooring lines, which are typically represented using either quasi-static or dynamic models, each suited for different stages of design according to Cruz and Atcheson [40].Quasi-static models, which assume the lines are in a state of equilibrium between the anchor and platform attachment point, are computationally efficient and useful for early-stage design but typically underestimate mooring tension and neglect dynamic effects like fluid drag, added mass, and nonlinear boundary interactions [40]. Dynamic models, though more computationally intensive, address these limitations and achieve greater accuracy by treating the mooring line as a series of kinematic elements that respond to varying loads, making them essential for detailed analysis in later design stages, especially under extreme conditions [40]. Specific dynamic models used in FOWT analysis include the finite difference model, finite segment model, finite element model, and lumped mass model [22]. Although dynamic models are more accurate, many fully coupled aero–hydro CFD simulations employ simpler mooring line models (i.e., quasi-static) to reduce computational costs and focus more on turbine–platform interactions (e.g., [11,115,118,119,123,127,132]). For a more accurate representation of the full system's dynamic responses, additional research should find ways to include more accurate mooring models.

5.1.3. Solver Settings

To set up the solver for the CFD model, the discretization method for approximating the derivatives in the NS equations must be specified. Typical methods include (1) the finite difference method (FDM), which uses approximations for the derivatives at the grid points; (2) the finite volume method (FVM), which uses approximations for the surface and volume integrals; and (3) FEM, which uses shape functions (elements) and weighting functions, more commonly used in structural analysis [5,23,137]. FVM is most commonly used in FOWT applications, since it can be applied to any type of grid and is most suitable for complex geometries. For more details on each of these methods, refer to Ferziger et al. [137]. Within the CFD solver, a scheme for imposing incompressibility (i.e., pressure–velocity coupling algorithms) is also necessary for these applications. The main pressure–velocity coupling schemes used in FOWT applications include SIMPLE (i.e., Semi-Implicit Methods' Pressure-Linked Equations) [115,127,132] and PISO (i.e., Pressure-Implicit with Splitting

of Operators) [113,122,123] schemes. These two methods can also be merged to form the PIMPLE scheme, which is used by Zhou et al. [120,124] in their fully coupled analysis of the OC4 DeepCWind semi-submersible.

Finally, the solver requires the identification of the specific advection scheme, which identifies how information is transferred across the domain. Refer to Ferziger et al. [137] for definitions of the possible options and the applicability of each.

The decisions of which numerical methods to use play a key role in the accuracy and computational cost of these fully coupled CFD simulations, and there is often a significant trade-off between the two. This necessitates future research in improving CFD modeling techniques to maintain accuracy, while also increasing computational efficiency so that these models can reach their full potential. Uncertainty and sensitivity studies are also necessary to test the effects of changing different model parameters [93].

6. Future Directions and Research Opportunities

As the reliance on floating offshore wind energy increases and the industry evolves, the application of CFD faces increasing challenges and opportunities. Based on combined findings from the literature, there are three main research areas that require attention in order to overcome the limitations of CFD: (1) improving model accuracy, (2) reducing computational expense, and (3) adapting models for new technological advancements.

6.1. Improving Model Accuracy

Developing accurate models is necessary to fully understand the loads and dynamic behavior of FOWT systems under the various hazards of the offshore environment. While CFD techniques are already the most accurate of the various FOWT modeling approaches, there is still room for improvement.

For example, uncertainty and sensitivity analyses are crucial for improving the accuracy of CFD models [15]. Sensitivity analyses help identify the most influential variables and their effects on the simulation outcomes. Notably, mesh sensitivity studies can be conducted by starting with a relatively coarse mesh and observing the impact on the results as the mesh density increases. Following sensitivity studies, the most relevant uncertainties can be quantified. Wang et al. [152] highlight three primary sources of uncertainty in CFD simulations: numerical uncertainties (e.g., round-off errors, iterative errors, and discretization errors), modeling uncertainties (e.g., turbulence model and boundary conditions), and statistical uncertainties (e.g., fluctuations from environmental loads). Among these, spatial discretization, i.e., mesh resolution, is often the dominant factor affecting the accuracy of CFD predictions. By understanding the inherent uncertainties and incorporating them into the optimization process, more reliable and robust CFD models can be developed that can accurately predict FOWT loads and system responses, even under varying environmental conditions [19,93].

The need for rigorous model validation and code-to-code comparisons is also critical for enhancing the accuracy and reliability of CFD modeling approaches [52]. As CFD models become increasingly complex, the reliability of their predictions hinges on thorough verification and validation processes. This involves using representative prototypes and respective experimental data as a benchmark, as discussed in Section 5. These datasets are essential for assessing the accuracy of CFD models and ensuring the applicability of prototypes in real-world scenarios; however, full-scale experimental data is still scarce and difficult to obtain [93]. In addition to experimental validation, code-to-code comparisons offer another critical method for verifying the predictive accuracy of numerical simulation tools. For example, collaborative efforts like the Offshore Code Comparison (OCC) projects have been instrumental in advancing offshore wind energy technology by enabling direct comparisons between different modeling approaches [92]. This project series began with the OC3 [94] and OC4 [153,154] projects, under IEA Wind Tasks 23 and 30, respectively. These projects ran from 2005–2013 and focused on verifying modeling tools via a code-to-code comparison of simulated responses from several different models. Following this

work, the OC5 project [101,155–158] was also created under Task 30. This project ran from 2014–2018 and focused on validating simulation results against real test data from the Alpha Ventus offshore wind farm. As an extension of previous Task 30 research, the OC6 project was conducted throughout 2019–2023. This project consists of four phases, focused on different aspects of FOWT design: phase I [102,159,160] considers the hydrodynamic response of floating support structures, especially the nonlinear low-frequency responses; phase II [161] considers soil/structure interaction; phase III [103,162] considers aerodynamic loading on a wind turbine rotor under motion; and phase IV [163] considers full-system hydrodynamic and aerodynamic interaction. Currently, the OC7 project is underway for a planned time-frame of 2024–2027, as part of a new Task 56. The main focus of this project includes (1) hydrodynamic modeling evolution, (2) the incorporation of structural flexibility, and (3) wind farm wake effects [164]. The ongoing process of validation and comparison is crucial for the continued development of reliable CFD models capable of accurately simulating the complex dynamics of FOWTs.

In improving CFD modeling techniques, additional consideration should be given to the availability and quality of metocean data (i.e., wind, wave and current information), which can heavily influence the accuracy of CFD simulations [165]. These data are crucial for understanding and predicting the complex environment that FOWTs operate under, especially during more frequent extreme weather events [165]. Thus, accurate metocean data are essential for optimizing the design, site selection, and operational planning of FOWTs, as it directly informs CFD models and thus the calculation of design loads. The integration of enhanced metocean data collection methods can therefore play a critical role in refining CFD models and improving the reliability of FOWT designs in diverse ocean environments and extreme conditions. [19,165].

6.2. Increasing Computational Efficiency

Despite the high accuracy and advanced capabilities of high-fidelity CFD modeling, their low computational efficiency (corresponding to high cost and time requirements) remains the largest drawback, especially for the extensive and long-duration simulations that are often necessary for realistic FOWT modeling. Therefore, a major research effort within the FOWT modeling community is in reducing the computational requirements of these simulations without compromising accuracy. Zhang et al [23] identify some innovative methods that have been developed to support this effort, including (a) multi-fidelity modeling, i.e., incorporating high-fidelity models earlier in the design process, (b) parallel computing and GPU acceleration, (c) reduced-order modeling (ROM), (d) adaptive mesh refinement, and (e) Lattice–Boltzmann methods, which are all described in more detail in their review.

In addition to these approaches, integration with machine learning (ML) techniques can also play a major role in increasing the computational efficiency of CFD models, particularly for highly turbulent flow and large computational domains [166]. Note that ML algorithms are a subclass of artificial intelligence (AI) with the ability to learn by extracting underlying patterns within a dataset without being explicitly programmed [167,168]. The learning process—which involves data collection and preparation, training, evaluation, and tuning—enables predictive modeling that can be leveraged in CFD simulations. Thus, research in this area has been growing rapidly in the last decade for general CFD applications (e.g., see reviews by Wang et al. [169], Vinuesa et al. [170], and Panchigar et al. [166]) and is gaining traction in the offshore wind research community as well [167,171], for a variety of applications.

Typical approaches for using ML for CFD applications include data-driven surrogates (which rely solely on observed data for training), physics-driven surrogates (which integrate physics-based priors to inform the model), and ML-assisted numerical solutions (which replace certain aspects of the numerical solver with ML models). These models are discussed in more detail by Wang et al. [169] and each have their own advantages and trade-offs.

Data-driven surrogates can either be dependent on discretization (i.e., the data domain is divided into a specific regular grid, irregular mesh or Lagrangian particle structure prior to design of the model architecture) or independent of discretization (i.e., it directly learns the solution in a continuous space) [169]. Based on the review by Barooni et al., common data-driven methods that can be used for dynamic analyses include Gaussian processes, support-vector networks, Wiener chaos expansion, decision networks, radial basis functions, dynamic mode decomposition, and neural networks (NNs) [9]. Data-driven models tend to be fast and efficient once trained, making them suitable for real-time predictions and optimization, but they require large, high-quality datasets to generalize well in unseen working conditions and may struggle with extrapolating beyond the training data [170]. On the other hand, physics-driven surrogates implement prior knowledge (such as initial conditions, boundary conditions and conservation laws) into NNs, and are categorized as either physics-informed (i.e., uses physical knowledge to constrain a NN) or constrained-informed (i.e., integrates inspiration from traditional PDE solvers into the NN training process) [169]. As identified by Vinuesa et al. [170], physics-informed neural networks (PINNs) are increasing in popularity, e.g., for turbulence modeling (solving RANS equations without a Reynolds stress model [172]), the development of ROMs [173], dealing with noisy data [174], and accelerating traditional solvers (such as obtaining a more efficient solution of the Poisson equation [175]). The integration of prior knowledge enables physics-driven surrogates to generalize better with less data while preserving physically consistent solutions, but they tend to be limited in terms of flexibility and scalability for large simulations.

In recent years, surrogate models have seen significant potential for advancing CFD simulation, but are still not as accurate as full numerical solvers and have limited applicability [166,169]. As an alternative, ML-assisted numerical solutions employ a hybrid approach that offers a balance between speed, accuracy and generalization. According to the review by Wang et al. [169], one application of these hybrid models involves learning discretization schemes and fluxes by generating space- and time-varying finite difference/volume coefficients that serve as corrections to the original coefficients to enable coarser mesh resolutions without compromising accuracy (note that normally, discretization errors increase as mesh resolution coarsens) [176–179]. While ML-assisted models offer great potential, ensuring stability and maintaining accuracy when integrating ML into established solvers remains a challenge and a source of future research.

Additionally, further exploration in how various ML approaches can be applied specifically for CFD simulations of FOWTs (e.g., for improved turbulence modeling) is necessary.

6.3. Adapting to New Technological Advancements

As FOWTs continue to scale up in size and complexity, adapting CFD models to keep pace with technological advancements is also crucial. The shift towards larger turbines with capacities exceeding 20 MW (e.g., the IEA 22 MW turbine [112]) and more complex floating platforms [28] introduces new challenges that existing CFD models must address. For instance, large rotor diameters bring about significant structural deformations that are not fully captured in current high-fidelity CFD frameworks [22].

Therefore, more research is needed in advancing fully coupled CFD models to accurately capture the complex interactions between aerodynamics, hydrodynamics, and structural dynamics, as introduced in Section 5. This can be achieved by integrating structural dynamic effects with aerodynamics and hydrodynamics via coupled CFD-FEM models [93]. These fully coupled CFD-FEM models are still in the early stages of development and require significant advancements before they can become more widely adopted in the industry, especially in addressing the computational inefficiencies associated with such complex simulations [23].

As turbines increase in size and slenderness, the reliance on control algorithms will also continue to grow. Controls play a crucial role in FOWT dynamic analysis for reducing structural vibrations, which mitigates unwanted stresses and fatigue, thus extending

turbine lifespan and lowering maintenance requirements [9]. Thus, another point of future research is in control co-design approaches [180], in which controls and the structure are designed simultaneously [19].

Moreover, as the floating offshore wind industry grows, extending CFD modeling capabilities from individual turbines to entire wind farms becomes essential, especially with innovative efforts towards larger wind farm layouts [181,182] and shared mooring systems [183,184]. Expanding CFD to model floating wind farms involves simulating interactions between multiple turbines, assessing the impacts on energy yield, and optimizing turbine placement to minimize wake effects [22]. In particular, multi-turbine CFD investigations need to be developed further in order to understand the physical mechanisms of wake interactions on downwind turbines and how it affects performance [22]. Additionally, the increased scale of FOWTs necessitates more accurate modeling of atmospheric inflow conditions, particularly through LES, to account for wind shear, turbulence, and wake effects, which are critical for predicting turbine performance and fatigue loads [22,185].

The integration of innovative multi-turbine floating platforms [19,186,187] and hybrid wind–wave platforms [19,188,189] also demand advancements in CFD models. In summary, the evolving floating wind landscape requires models that not only accommodate the growing scale and complexity of FOWTs but also incorporate new design innovations, ensuring the accuracy and reliability of fully coupled CFD simulations.

7. Conclusions

Floating offshore wind is expected to play a critical role in the global clean energy transition and contribute towards reaching necessary sustainability goals. Despite the remarkable progress made in developing new floating platform designs and advanced numerical models to simulate the complex dynamics of FOWTs, the technology is still in its nascent stages. Most notably, the dynamic challenges posed by the harsh offshore environment necessitate continued research and innovation.

Fully coupled CFD modeling plays a key role in achieving the cost reductions and design confidence necessary for floating wind to fully establish itself as a reliable and practical renewable energy technology. In particular, FOWT designers are increasingly turning to these advanced numerical tools to (1) reduce reliance on expensive and time-consuming physical model tests, (2) minimize uncertainties inherent in simpler, lower-fidelity, numerical models, and (3) achieve more accurate predictions of FOWT behaviors under realistic conditions, especially under isolated extreme weather events.

While fully coupled CFD has the opportunity to offer highly accurate and predictive results for FOWT applications, these simulations require significant computational resources and are quite comprehensive compared to simpler models, so researchers must be intentional about the simulations that they conduct. In particular, the pre-processing stage of the CFD modeling process involves a plethora of decisions for which numerical methods to employ, including how the mesh is constructed and treated in the presence of the free surface, how to define key physical aspects (e.g., boundary conditions, turbulence, interface treatment, moorings, rotor, etc.), and which solver settings to employ (e.g., discretization method, advection scheme, pressure–velocity coupling scheme, etc.). These decisions have a large influence on the accuracy and efficiency of CFD simulations and there is often a significant trade-off between the two. In many cases, accuracy is compromised for simplicity and lower computational costs, identifying a major barrier for CFD simulations.

Therefore, in order for fully coupled CFD modeling to reach its full potential, it is necessary to increase research efforts in improving the efficiency of these models without compromising accuracy. In particular, there is increasing interest in (1) uncertainty and sensitivity analyses to test the effects of changing different model parameters, and (2) the implementation of machine learning methods to reduce simulation time. Additionally, adapting CFD models to keep pace with technological advancements (e.g., larger turbines, more complex platforms, larger wind farm layouts, shared mooring systems, etc.) is also necessary.

Advanced research efforts in these areas will play a crucial role in overcoming existing limitations and ensuring reliable, predictive, and cost-effective FOWT modeling capability as the industry continues to evolve.

Author Contributions: Conceptualization, H.D. and D.P.S.; investigation, H.D.; writing—original draft preparation, H.D.; writing—review and editing, H.D. and D.P.S.; supervision, D.P.S. All authors have read and agreed to the published version of the manuscript.

Funding: This research is supported in part by National Science Foundation grants 2020888 and 2021693.

Conflicts of Interest: The authors declare no conflicts of interest.

References

1. IPCC. 2023: Sections. In *Climate Change 2023: Synthesis Report. Contribution of Working Groups I, II and III to the Sixth Assessment Report of the Intergovernmental Panel on Climate Change*; Core Writing Team, Lee, H., Romero, J. Eds.; IPCC: Geneva, Switzerland, 2023; pp. 35–115. [CrossRef]
2. Veers, P.; Dykes, K.; Baranowski, R.; Bay, C.; Bortolotti, P.; Doubrawa, P.; MacDonald, S.; Rooney, S.; Bottasso, C.L.; Fleming, P.; et al. *Grand Challenges Revisited: Wind Energy Research Needs for a Global Energy Transition*; Technical report; National Renewable Energy Laboratory (NREL): Golden, CO, USA, 2023.
3. Stéphanie, B.; Araceli Fernandez, P.; Christophe, M.; Uwe, R.; Brent, W.; Laszlo, V.; Davide, D.; Thomas, S. *Net Zero by 2050: A Roadmap for the Global Energy Sector*; OECD Publishing: Paris, France. 2021.
4. IRENA. *Tracking COP28 Outcomes: Tripling Renewable Power Capacity by 2030*; International Renewable Energy Agency: Abu Dhabi, United Arab Emirates, 2024.
5. Shourangiz-Haghighi, A.; Haghnegahdar, M.A.; Wang, L.; Mussetta, M.; Kolios, A.; Lander, M. State of the art in the optimisation of wind turbine performance using CFD. *Arch. Comput. Methods Eng.* **2020**, *27*, 413–431. [CrossRef]
6. Liu, T.; Tavner, P.; Feng, Y.; Qiu, Y. Review of recent offshore wind power developments in china. *Wind Energy* **2013**, *16*, 786–803. [CrossRef]
7. Bazmi, A.A.; Zahedi, G. Sustainable energy systems: Role of optimization modeling techniques in power generation and supply—A review. *Renew. Sustain. Energy Rev.* **2011**, *15*, 3480–3500. [CrossRef]
8. Lead Authors: Lee, J.; Zhao, F. *GWEC Global Wind Report 2024*; Global Wind Energy Council: Brussels, Belgium, 2024.
9. Barooni, M.; Ashuri, T.; Velioglu Sogut, D.; Wood, S.; Ghaderpour Taleghani, S. Floating offshore wind turbines: Current status and future prospects. *Energies* **2022**, *16*, 2. [CrossRef]
10. Asim, T.; Islam, S.Z.; Hemmati, A.; Khalid, M.S.U. A review of recent advancements in offshore wind turbine technology. *Energies* **2022**, *15*, 579. [CrossRef]
11. Liu, Y.; Xiao, Q.; Incecik, A.; Peyrard, C.; Wan, D. Establishing a fully coupled CFD analysis tool for floating offshore wind turbines. *Renew. Energy* **2017**, *112*, 280–301. [CrossRef]
12. Díaz, H.; Soares, C.G. Review of the current status, technology and future trends of offshore wind farms. *Ocean Eng.* **2020**, *209*, 107381. [CrossRef]
13. Arapogianni, A.; Genachte, A.; Ochagavia, R.; Vergara, J.; Castell, D.; Tsouroukdissian, A.; Korbijn, J.; Bolleman, N.; Huera-Huarte, F.; Schuon, F.; et al. *Deep Water—The Next Step for Offshore Wind Energy*; European Wind Energy Association (EWEA): Brussels, Belgium. 2013; pp. 978–972.
14. O'Kelly, B.; Arshad, M. Offshore wind turbine foundations–analysis and design. In *Offshore Wind Farms*; Elsevier: Amsterdam, The Netherlands, 2016; pp. 589–610.
15. Zeng, X.; Shao, Y.; Feng, X.; Xu, K.; Jin, R.; Li, H. Nonlinear hydrodynamics of floating offshore wind turbines: A review. *Renew. Sustain. Energy Rev.* **2024**, *191*, 114092. [CrossRef]
16. Wind Energy Technologies Office; *Floating Offshore Wind Shot: Unlocking the Power of Floating Offshore Wind Energy*; Energy Earthshots U.S. Department of Energy: 2022.
17. Mills, S.B.; Bessette, D.; Smith, H. Exploring landowners' post-construction changes in perceptions of wind energy in Michigan. *Land Use Policy* **2019**, *82*, 754–762. [CrossRef]
18. Schallenberg-Rodríguez, J.; Montesdeoca, N.G. Spatial planning to estimate the offshore wind energy potential in coastal regions and islands. Practical case: The Canary Islands. *Energy* **2018**, *143*, 91–103. [CrossRef]
19. Subbulakshmi, A.; Verma, M.; Keerthana, M.; Sasmal, S.; Harikrishna, P.; Kapuria, S. Recent advances in experimental and numerical methods for dynamic analysis of floating offshore wind turbines—An integrated review. *Renew. Sustain. Energy Rev.* **2022**, *164*, 112525. [CrossRef]
20. Otter, A.; Murphy, J.; Pakrashi, V.; Robertson, A.; Desmond, C. A review of modelling techniques for floating offshore wind turbines. *Wind Energy* **2022**, *25*, 831–857. [CrossRef]
21. Chen, P.; Chen, J.; Hu, Z. Review of experimental-numerical methodologies and challenges for floating offshore wind turbines. *J. Mar. Sci. Appl.* **2020**, *19*, 339–361. [CrossRef]

22. Xu, S.; Xue, Y.; Zhao, W.; Wan, D. A Review of High-Fidelity Computational Fluid Dynamics for Floating Offshore Wind Turbines. *J. Mar. Sci. Eng.* **2022**, *10*, 1357. [CrossRef]
23. Zhang, W.; Calderon-Sanchez, J.; Duque, D.; Souto-Iglesias, A. Computational Fluid Dynamics (CFD) applications in Floating Offshore Wind Turbine (FOWT) dynamics: A review. *Appl. Ocean Res.* **2024**, *150*, 104075. [CrossRef]
24. Haider, R.; Li, X.; Shi, W.; Lin, Z.; Xiao, Q.; Zhao, H. Review of computational fluid dynamics in the design of floating offshore wind turbines. *Energies* **2024**, *17*, 4269. [CrossRef]
25. Heronemus, W.E. Pollution-free energy from offshore winds. In Proceedings of the 8th Annual Conference and Exposition, Marine Technology Society, Washington, DC, USA, 11–13 September 1972.
26. Stoddard, W. The Life and Work of Bill Heronemus, wind engineering pioneer. *Wind Eng.* **2002**, *26*, 335–341. [CrossRef]
27. Butterfield, S.; Musial, W.; Jonkman, J.; Sclavounos, P. *Engineering Challenges for Floating Offshore Wind Turbines*; Technical report, National Renewable Energy Lab. (NREL): Golden, CO, USA, 2007.
28. Edwards, E.C.; Holcombe, A.; Brown, S.; Ransley, E.; Hann, M.; Greaves, D. Trends in floating offshore wind platforms: A review of early-stage devices. *Renew. Sustain. Energy Rev.* **2024**, *193*, 114271. [CrossRef]
29. Mei, X.; Xiong, M. Effects of second-order hydrodynamics on the dynamic responses and fatigue damage of a 15 MW floating offshore wind turbine. *J. Mar. Sci. Eng.* **2021**, *9*, 1232. [CrossRef]
30. Castro-Santos, L.; Diaz-Casas, V. *Floating Offshore Wind Farms*; Springer: Berlin/Heidelberg, Germany, 2016.
31. Savenije, L.; Ashuri, T.; Bussel, G.; Staerdahl, J. Dynamic modeling of a spar-type floating offshore wind turbine. In Proceedings of the European Wind Energy Conference and Exhibition (EWEC), Warsaw, Poland, 20–23 April 2010; pp. 20–23.
32. Equinor. Hywind Scotland. 2021. Available online: https://www.equinor.com/energy/hywind-scotland (accessed on 24 September 2024).
33. Windplus. WindFloat Atlantic. 2020. Available online: www.windfloat-atlantic.com (accessed on 24 September 2024).
34. Principle Power. Kincardine. 2021. Available online: www.principlepower.com/projects/kincardine-offshore-wind-farm (accessed on 24 September 2024).
35. Equinor. Hywind Tampen. 2022. Available online: www.equinor.com/energy/hywind-tampen (accessed on 24 September 2024).
36. Musial, W.; Spitsen, P.; Duffy, P.; Beiter, P.; Shields, M.; Mulas Hernando, D.; Hammond, R.; Marquis, M.; King, J.; Sathish, S. *Offshore Wind Market Report: 2023 Edition*; Technical report; National Renewable Energy Laboratory (NREL): Golden, CO, USA; 2023.
37. Hu, D.; Deng, L.; Zeng, L. Study on the aerodynamic performance of floating offshore wind turbine considering the tower shadow effect. *Processes* **2021**, *9*, 1047. [CrossRef]
38. Cottura, L.; Caradonna, R.; Novo, R.; Ghigo, A.; Bracco, G.; Mattiazzo, G. Effect of pitching motion on production in a OFWT. *J. Ocean Eng. Mar. Energy* **2022**, *8*, 319–330. [CrossRef]
39. Nielsen, F.G. *Offshore Wind Energy: Environmental Conditions and Dynamics of Fixed and Floating Turbines*; Cambridge University Press: Cambridge, UK , 2024.
40. Cruz, J.; Atcheson, M. *Floating Offshore Wind Energy: The Next Generation of Wind Energy*; Springer International Publishing: Cham, Switzerland , 2016.
41. Ranta, J.; Polojärvi, A. Limit mechanisms for ice loads on inclined structures: Local crushing. *Mar. Struct.* **2019**, *67*, 102633. [CrossRef]
42. Sirnivas, S.; Musial, W.; Bailey, B.; Filippelli, M. *Assessment of Offshore Wind System Design, Safety, and Operation Standards*; Technical Report; National Renewable Energy Lab. (NREL): Golden, CO, USA, 2014.
43. Karimirad, M. *Offshore Energy Structures: For Wind Power, Wave Energy and Hybrid Marine Platforms*; Springer: Berlin/Heidelberg, Germany, 2014.
44. Manwell, J.F.; McGowan, J.G.; Rogers, A.L. *Wind Energy Explained: Theory, Design and Application*; John Wiley & Sons: Hoboken, NJ, USA , 2010.
45. Leishman, J.G. Challenges in modelling the unsteady aerodynamics of wind turbines. *Wind Energy Int. J. Prog. Appl. Wind Power Convers. Technol.* **2002**, *5*, 85–132. [CrossRef]
46. Huyer, S.A.; Simms, D.; Robinson, M.C. Unsteady aerodynamics associated with a horizontal-axis wind turbine. *AIAA J.* **1996**, *34*, 1410–1419. [CrossRef]
47. Robinson, M.; Galbraith, R.; Shipley, D.; Miller, M. Unsteady aerodynamics of wind turbines. In Proceedings of the 33rd Aerospace Sciences Meeting and Exhibit, Reno, NV, USA, 9–12 January 1995; p. 526.
48. Cai, Y.; Zhao, H.; Li, X.; Liu, Y. Effects of yawed inflow and blade-tower interaction on the aerodynamic and wake characteristics of a horizontal-axis wind turbine. *Energy* **2023**, *264*, 126246. [CrossRef]
49. Chanprasert, W.; Sharma, R.; Cater, J.; Norris, S. Large Eddy Simulation of wind turbine wake interaction in directionally sheared inflows. *Renew. Energy* **2022**, *201*, 1096–1110. [CrossRef]
50. Rezaeiha, A.; Micallef, D. Wake interactions of two tandem floating offshore wind turbines: CFD analysis using actuator disc model. *Renew. Energy* **2021**, *179*, 859–876. [CrossRef]
51. Zhou, Y.; Xiao, Q.; Liu, Y.; Incecik, A.; Peyrard, C.; Wan, D.; Pan, G.; Li, S. Exploring inflow wind condition on floating offshore wind turbine aerodynamic characterisation and platform motion prediction using blade resolved CFD simulation. *Renew. Energy* **2022**, *182*, 1060–1079. [CrossRef]

52. Matha, D.; Schlipf, M.; Pereira, R.; Jonkman, J. Challenges in simulation of aerodynamics, hydrodynamics, and mooring-line dynamics of floating offshore wind turbines. In Proceedings of the 21st International Offshore and Polar Engineering Conference, Maui, HI, USA, 19–24 June 2011; p. ISOPE–I.
53. Sebastian, T.; Lackner, M. Characterization of the unsteady aerodynamics of offshore floating wind turbines. *Wind Energy* **2013**, *16*, 339–352. [CrossRef]
54. Tran, T.T.; Kim, D.H. The platform pitching motion of floating offshore wind turbine: A preliminary unsteady aerodynamic analysis. *J. Wind Eng. Ind. Aerodyn.* **2015**, *142*, 65–81. [CrossRef]
55. Lynn, P.A. *Onshore and Offshore Wind Energy: An Introduction*; John Wiley & Sons: Hoboken, NJ, USA, 2011.
56. Williamson, C.H.; Govardhan, R. Vortex-induced vibrations. *Annu. Rev. Fluid Mech.* **2004**, *36*, 413–455. [CrossRef]
57. Benitz, M.A.; Lackner, M.; Schmidt, D. Hydrodynamics of offshore structures with specific focus on wind energy applications. *Renew. Sustain. Energy Rev.* **2015**, *44*, 692–716. [CrossRef]
58. Thiagarajan, K.; Dagher, H. A review of floating platform concepts for offshore wind energy generation. *J. Offshore Mech. Arct. Eng.* **2014**, *136*, 020903. [CrossRef]
59. Sound and Sea Technology. *Advanced Anchoring and Mooring Study*; Technical Report; Oregon Wave Energy Trust (OWET): Portland, OR, USA, 2009.
60. Rui, S.; Zhou, Z.; Gao, Z.; Jostad, H.P.; Wang, L.; Xu, H.; Guo, Z. A review on mooring lines and anchors of floating marine structures. *Renew. Sustain. Energy Rev.* **2024**, *199*, 114547. [CrossRef]
61. Lamei, A.; Hayatdavoodi, M. On motion analysis and elastic response of floating offshore wind turbines. *J. Ocean Eng. Mar. Energy* **2020**, *6*, 71–90. [CrossRef]
62. Robertson, A.; Jonkman, J.; Goupee, A.; Coulling, A.; Prowell, I.; Browning, J.; Masciola, M.; Molta, P. Summary of conclusions and recommendations drawn from the DeepCwind scaled floating offshore wind system test campaign. *Am. Soc. Mech. Eng. Int. Conf. Offshore Mech. Arct. Eng.* **2013**, *55423*, V008T09A053.
63. Müller, K.; Sandner, F.; Bredmose, H.; Azcona, J.; Manjock, A.; Pereira, R. *Improved Tank Test Procedures for Scaled Floating Offshore Wind Turbines*; University of Stuttgart: Stuttgart, Germany, 2014.
64. Stewart, G.; Muskulus, M. A review and comparison of floating offshore wind turbine model experiments. *Energy Procedia* **2016**, *94*, 227–231. [CrossRef]
65. Gueydon, S.; Bayati, I.; De Ridder, E. Discussion of solutions for basin model tests of FOWTs in combined waves and wind. *Ocean Eng.* **2020**, *209*, 107288. [CrossRef]
66. Edition, F.; Journée, J.; Massie, W. *Offshore Hydromechanics*; Delft University of Technology: Delft, The Netherlands, 2001.
67. Barltrop, N.D.P. *Floating Structures: A Guide for Design and Analysis*; Energy Institute: London, UK , 1998.
68. Yu, W.; Müller, K.; Lemmer, F. Qualification of innovative floating substructures for 10 MW wind turbines and water depths greater than 50 m. *LIFES50* **2018**. [CrossRef]
69. Hegseth, J.M.; Bachynski, E.E. A semi-analytical frequency domain model for efficient design evaluation of spar floating wind turbines. *Mar. Struct.* **2019**, *64*, 186–210. [CrossRef]
70. Karimi, M.; Hall, M.; Buckham, B.; Crawford, C. A multi-objective design optimization approach for floating offshore wind turbine support structures. *J. Ocean Eng. Mar. Energy* **2017**, *3*, 69–87. [CrossRef]
71. Pegalajar-Jurado, A.; Borg, M.; Bredmose, H. An efficient frequency-domain model for quick load analysis of floating offshore wind turbines. *Wind Energy Sci.* **2018**, *3*, 693–712. [CrossRef]
72. Hall, M.; Housner, S.; Zalkind, D.; Bortolotti, P.; Ogden, D.; Barter, G. An open-source frequency-domain model for floating wind turbine design optimization. *J. Physics Conf. Ser.* **2022**, *2265-4*, 042020. [CrossRef]
73. NREL. OpenFAST n.d. Available online: www.nrel.gov/wind/nwtc/openfast.html (accessed on 24 September 2024).
74. Jonkman, J.M.; Wright, A.D.; Hayman, G.J.; Robertson, A.N. Full-system linearization for floating offshore wind turbines in OpenFAST. In Proceedings of the International Conference on Offshore Mechanics and Arctic Engineering. American Society of Mechanical Engineers, Madrid, Spain, 17–22 June 2018; Volume 51975, p. V001T01A028.
75. DTU Wind. HAWC2 n.d. Available online: www.hawc2.dk (accessed on 24 September 2024).
76. SINTEF Ocean. SIMA. n.d. Available online: www.sintef.no/en/software/sima (accessed on 24 September 2024).
77. DNV. Bladed n.d. Available online: https://www.dnv.com/services/wind-turbine-design-software-bladed-3775 (accessed on 24 September 2024).
78. Dassault Systems. SIMPACK Multibody System Simulation Software n.d. Available online: www.3ds.com/products/simulia/simpack/wind (accessed on 24 September 2024).
79. Orcina. Orcaflex n.d. Available online: www.orcina.com/orcaflex (accessed on 24 September 2024).
80. Wood Group. Flexcom n.d. Available online: www.woodplc.com/solutions/expertise/flexcom (accessed on 24 September 2024).
81. OpenFOAM, The OpenFOAM Foundation, 2024. Available online: www.openfoam.org (accessed on 24 September 2024).
82. OpenFOAM, OpenCFD Limited, 2024. Available online: www.openfoam.com (accessed on 24 September 2024).
83. StarCCM+, Siemens Simcenter, 2024. Available online: plm.sw.siemens.com/en-US/simcenter/fluids-thermal-simulation/star-ccm (accessed on 24 September 2024).
84. Ansys Fluent, Ansys, 2024. Available online: www.ansys.com/products/fluids/ansys-fluent (accessed on 24 September 2024).
85. CONVERGE CFD Software, Convergent Science Inc, 2024. Available online: https://convergecfd.com (accessed on 24 September 2024).

86. Helicopter Multi-Block Code. 2024. ARCHIE-WeSt. University of Glasgow. Available online: www.archie-west.ac.uk/projects/computational-fluid-dynamics/helicopter-multi-block-code/ (accessed on 24 September 2024).
87. ReFRESCO, MARIN, 2024. Available online: www.marin.nl/en/about/facilities-and-tools/software/refresco (accessed on 24 September 2024).
88. CFDShip-Iowa. The University of Iowa, 2024. Stern Lab. Available online: https://stern.lab.uiowa.edu/cfd-code (accessed on 24 September 2024).
89. Van Bussel, G.J.W. The Aerodynamics of Horizontal axis Wind Turbine Rotors Explored with Asymptotic Expansion Methods. Ph.D. Thesis, Technische Universiteit Delft, Delft, The Netherlands, 1995.
90. Glauert, H. Airplane Propellers. In *Aerodynamic Theory*; Springer: Berlin/Heidelberg, Germany, 1935.
91. Fadaei, S.; Afagh, F.F.; Langlois, R.G. A survey of numerical simulation tools for offshore wind turbine systems. *Wind* **2024**, *4*, 1–24. [CrossRef]
92. Cordle, A.; Jonkman, J. State of the art in floating wind turbine design tools. In Proceedings of the ISOPE International Ocean and Polar Engineering Conference, Maui, HI, USA, 19–24 June 2011 ; ISOPE: Mountain View, CA, USA , 2011; p. ISOPE–I.
93. Maali Amiri, M.; Shadman, M.; Estefen, S.F. A Review of Numerical and Physical Methods for Analyzing the Coupled Hydro–Aero–Structural Dynamics of Floating Wind Turbine Systems. *J. Mar. Sci. Eng.* **2024**, *12*, 392. [CrossRef]
94. Jonkman, J.; Musial, W. *Offshore Code Comparison Collaboration (OC3) for IEA Wind Task 23 Offshore Wind Technology and Deployment*; Technical report; National Renewable Energy Lab. (NREL): Golden, CO, USA, 2010.
95. COREWIND, 2024. WindCrete. Available online: www.windcrete.com (accessed on 24 September 2024).
96. Molins, C.; Yagüe, A.; Trubat, P. Construction possibilities for monolithic concrete spar buoy serial production. *J. Physics Conf. Ser. IOP* **2018**, *1104-1*, 012020. [CrossRef]
97. Mahfouz, M.Y.; Molins, C.; Trubat, P.; Hernández, S.; Vigara, F.; Pegalajar-Jurado, A.; Bredmose, H.; Salari, M. Response of the International Energy Agency (IEA) Wind 15 MW WindCrete and Activefloat floating wind turbines to wind and second-order waves. *Wind Energy Sci.* **2021**, *6*, 867–883. [CrossRef]
98. Coulling, A.J.; Goupee, A.J.; Robertson, A.N.; Jonkman, J.M.; Dagher, H.J. Validation of a FAST semi-submersible floating wind turbine numerical model with DeepCwind test data. *J. Renew. Sustain. Energy* **2013**, *5*, 023116. [CrossRef]
99. Robertson, A.; Jonkman, J.; Masciola, M.; Song, H.; Goupee, A.; Coulling, A.; Luan, C. *Definition of the Semisubmersible Floating System for Phase II of OC4*; Technical report; National Renewable Energy Lab. (NREL): Golden, CO, USA, 2014.
100. Robertson, A.; Jonkman, J.; Wendt, F.; Goupee, A.; Dagher, H. Definition of the OC5 DeepCwind semisubmersible floating system. *National Renewable Energy Laboratory, University of Maine* 2016. Available online: ttps://a2e.energy.gov/api/datasets/oc5/oc5.phase2/files/oc5.phase2.model.definition-semisubmersible-floating-system-phase2-oc5-ver15.pdf (accessed on 24 September 2024).
101. Robertson, A.N.; Wendt, F.; Jonkman, J.M.; Popko, W.; Dagher, H.; Gueydon, S.; Qvist, J.; Vittori, F.; Azcona, J.; Uzunoglu, E.; et al. OC5 project Phase II: Validation of global loads of the DeepCwind floating semisubmersible wind turbine. *Energy Procedia* **2017**, *137*, 38–57. [CrossRef]
102. Wang, L.; Robertson, A.; Jonkman, J.; Kim, J.; Shen, Z.R.; Koop, A.; Borràs Nadal, A.; Shi, W.; Zeng, X.; Ransley, E.; et al. OC6 Phase Ia: CFD simulations of the free-decay motion of the DeepCwind semisubmersible. *Energies* **2022**, *15*, 389. [CrossRef]
103. Bergua, R.; Robertson, A.; Jonkman, J.; Branlard, E.; Fontanella, A.; Belloli, M.; Schito, P.; Zasso, A.; Persico, G.; Sanvito, A.; et al. OC6 project Phase III: Validation of the aerodynamic loading on a wind turbine rotor undergoing large motion caused by a floating support structure. *Wind Energy Sci.* **2023**, *8*, 465–485. [CrossRef]
104. Wiley, W.; Bergua, R.; Robertson, A.; Jonkman, J.; Wang, L.; Borg, M.; Fowler, M. *Definition of the Stiesdal Offshore TetraSpar Floating Wind System for OC6 Phase IV*; Technical report; National Renewable Energy Laboratory (NREL): Golden, CO, USA, 2023.
105. Allen, C.; Viscelli, A.; Dagher, H.; Goupee, A.; Gaertner, E.; Abbas, N.; Hall, M.; Barter, G. *Definition of the UMaine VolturnUS-S Reference Platform Developed for the IEA Wind 15-Megawatt Offshore Reference Wind Turbine*; Technical report; National Renewable Energy Lab. (NREL): Golden, CO, USA; University of Maine: Orono, ME, USA , 2020.
106. Bachynski, E.E.; Moan, T. Design considerations for tension leg platform wind turbines. *Mar. Struct.* **2012**, *29*, 89–114. [CrossRef]
107. Jonkman, J.M. *Dynamics Modeling and Loads Analysis of an Offshore Floating Wind Turbine*; Technical report; National Renewable Energy Laboratory (NREL): Golden, CO, USA, 2007.
108. Vijfhuizen, W. Design of a Wind and Wave Power Barge. Master's Thesis, Department of Naval Architecture and Mechanical Engineering, Universities of Glasgow and Strathclyde, Glasgow, Scotland, 2006.
109. Jonkman, J. *Definition of a 5-MW Reference Wind Turbine for Offshore System Development*; National Renewable Energy Lab. (NREL): Golden, CO, USA, 2009.
110. Bak, C.; Zahle, F.; Bitsche, R.; Kim, T.; Yde, A.; Henriksen, L.C.; Hansen, M.H.; Blasques, J.P.A.A.; Gaunaa, M.; Natarajan, A. The DTU 10-MW reference wind turbine. In Proceedings of the Danish Wind Power Research 2013, Fredericia, Denmark, 27–28 May 2013.
111. Gaertner, E.; Rinker, J.; Sethuraman, L.; Zahle, F.; Anderson, B.; Barter, G.; Abbas, N.; Meng, F.; Bortolotti, P.; Skrzypinski, W.; et al. *Definition of the IEA 15-Megawatt Offshore Reference Wind Turbine*; National Renewable Energy Lab. (NREL): Golden, CO, USA, 2020.

112. Zahle, F.; Barlas, T.; Lonbaek, K.; Bortolotti, P.; Zalkind, D.; Wang, L.; Labuschagne, C.; Sethuraman, L.; Barter, G. *Definition of the IEA Wind 22-Megawatt Offshore Reference Wind Turbine*; Technical report; National Renewable Energy Laboratory (NREL): Golden, CO, USA, 2024.
113. Ren, N.; Li, Y.; Ou, J. Coupled wind-wave time domain analysis of floating offshore wind turbine based on Computational Fluid Dynamics method. *J. Renew. Sustain. Energy* **2014**, *6*, 023106. [CrossRef]
114. Quallen, S.; Xing, T. CFD simulation of a floating offshore wind turbine system using a variable-speed generator-torque controller. *Renew. Energy* **2016**, *97*, 230–242. [CrossRef]
115. Tran, T.T.; Kim, D.H. Fully coupled aero-hydrodynamic analysis of a semi-submersible FOWT using a dynamic fluid body interaction approach. *Renew. Energy* **2016**, *92*, 244–261. [CrossRef]
116. Leble, V.; Barakos, G. Demonstration of a coupled floating offshore wind turbine analysis with high-fidelity methods. *J. Fluids Struct.* **2016**, *62*, 272–293. [CrossRef]
117. Li, P.; Wan, D.; Hu, C. Fully-coupled dynamic response of a semi-submerged floating wind turbine system in wind and waves. In Proceedings of the ISOPE International Ocean and Polar Engineering Conference, Rhodes, Greece, 26 June–1 July 2016; ISOPE: Mountain View, CA, USA , 2016; p. ISOPE–I.
118. Tran, T.T.; Kim, D.H. A CFD study of coupled aerodynamic-hydrodynamic loads on a semisubmersible floating offshore wind turbine. *Wind Energy* **2018**, *21*, 70–85. [CrossRef]
119. Zhang, Y.; Kim, B. A fully coupled computational fluid dynamics method for analysis of semi-submersible floating offshore wind turbines under wind-wave excitation conditions based on OC5 data. *Appl. Sci.* **2018**, *8*, 2314. [CrossRef]
120. Zhou, Y.; Xiao, Q.; Liu, Y.; Incecik, A.; Peyrard, C.; Li, S.; Pan, G. Numerical modelling of dynamic responses of a floating offshore wind turbine subject to focused waves. *Energies* **2019**, *12*, 3482. [CrossRef]
121. Huang, Y.; Wan, D. Investigation of interference effects between wind turbine and spar-type floating platform under combined wind-wave excitation. *Sustainability* **2019**, *12*, 246. [CrossRef]
122. Huang, Y.; Cheng, P.; Wan, D. Numerical analysis of a floating offshore wind turbine by coupled aero-hydrodynamic simulation. *J. Mar. Sci. Appl.* **2019**, *18*, 82–92. [CrossRef]
123. Cheng, P.; Huang, Y.; Wan, D. A numerical model for fully coupled aero-hydrodynamic analysis of floating offshore wind turbine. *Ocean Eng.* **2019**, *173*, 183–196. [CrossRef]
124. Zhou, Y.; Xiao, Q.; Peyrard, C.; Pan, G. Assessing focused wave applicability on a coupled aero-hydro-mooring FOWT system using CFD approach. *Ocean Eng.* **2021**, *240*, 109987. [CrossRef]
125. Zheng, J.; Huang, Y.; Wan, D. Numerical Study of Coupled Aero-Hydrodynamics Performances of a Floating Offshore Wind Turbine with Heave Plate. In Proceedings of the ISOPE International Ocean and Polar Engineering Conference, Rhodes, Greece, 20–25 June 2021 ; ISOPE: Mountain View, CA, USA, 2021; p. ISOPE–I.
126. Xie, S.; Sadique, J. CFD Simulations of Two Tandem Semi-Submersible Floating Offshore Wind Turbines Using a Fully-Coupled Fluid-Structure-Interaction Simulation Methodology. In Proceedings of the International Conference on Offshore Mechanics and Arctic Engineering, Hamburg, Germany, 5–10 June 2022 ; American Society of Mechanical Engineers: New York City, USA 2022; Volume 86618, p. V001T01A006.
127. Huang, H.; Liu, Q.; Yue, M.; Miao, W.; Wang, P.; Li, C. Fully coupled aero-hydrodynamic analysis of a biomimetic fractal semi-submersible floating offshore wind turbine under wind-wave excitation conditions. *Renew. Energy* **2023**, *203*, 280–300. [CrossRef]
128. Huang, Y.; Zhao, W.; Wan, D. Wake interaction between two spar-type floating offshore wind turbines under different layouts. *Phys. Fluids* **2023**, *35*, 097102. [CrossRef]
129. Yu, Z.; Zheng, X.; Yuan, Y. Analysis of the blade aeroelastic effect on the floating offshore wind turbine wake in a focusing wave with a hybrid model. *Eng. Appl. Comput. Fluid Mech.* **2023**, *17*, 2260470. [CrossRef]
130. Yu, Z.; Ma, Q.; Zheng, X.; Liao, K.; Sun, H.; Khayyer, A. A hybrid numerical model for simulating aero-elastic-hydro-mooring-wake dynamic responses of floating offshore wind turbine. *Ocean Eng.* **2023**, *268*, 113050. [CrossRef]
131. Feng, X.; Fang, J.; Lin, Y.; Chen, B.; Li, D.; Liu, H.; Gu, Y. Coupled aero-hydro-mooring dynamic analysis of floating offshore wind turbine under blade pitch motion. *Phys. Fluids* **2023**, *35*, 045131.
132. Alkhabbaz, A.; Hamza, H.; Daabo, A.M.; Yang, H.S.; Yoon, M.; Koprulu, A.; Lee, Y.H. The aero-hydrodynamic interference impact on the NREL 5-MW floating wind turbine experiencing surge motion. *Ocean Eng.* **2024**, *295*, 116970. [CrossRef]
133. Sadique, J.; Xie, S.; Shekhawat, Y.; Darling, H.; Schmidt, D. Numerical Assessment and Validation of Floating Offshore Wind Turbines in One Fully Coupled CFD Simulation. In Proceedings of the Offshore Technology Conference Asia, Kuala Lumpur, Malaysia, 27 February–1 March 2024; p. D031S037R001.
134. Yu, Z.; Hu, Z.; Zheng, X.; Ma, Q.; Hao, H. Aeroelastic performance analysis of wind turbine in the wake with a new Elastic Actuator Line model. *Water* **2020**, *12*, 1233. [CrossRef]
135. Santo, G.; Peeters, M.; Van Paepegem, W.; Degroote, J. Fluid–structure interaction simulations of a wind gust impacting on the blades of a large horizontal axis wind turbine. *Energies* **2020**, *13*, 509. [CrossRef]
136. Miao, W.; Li, C.; Wang, Y.; Xiang, B.; Liu, Q.; Deng, Y. Study of adaptive blades in extreme environment using fluid–structure interaction method. *J. Fluids Struct.* **2019**, *91*, 102734. [CrossRef]
137. Ferziger, J.H.; Perić, M.; Street, R.L. *Computational Methods for Fluid Dynamics*; Springer Nature Switzerland AG: Cham, Switzerland, 2020.

138. OpenFOAM 2.1.0: Arbitrary Mesh Interface. 2011. The OpenFOAM Foundation. Available online: https://openfoam.org/release/2-1-0/ami (accessed on 24 September 2024).
139. Muzaferija, S. Computation of free surface flows using interface-tracking and interface-capturing methods. In *Nonlinear Water-Wave Interaction*; Computational Mechanics Publications, WIT Press: Southamption, UK, 1998.
140. Bertram, V. *Practical Ship Hydrodynamics*; Elsevier Ltd: Amsterdam, The Netherlands, 2012.
141. Hirt, C.W.; Nichols, B.D. Volume of fluid (VOF) method for the dynamics of free boundaries. *J. Comput. Phys.* **1981**, *39*, 201–225. [CrossRef]
142. Hou, G.; Wang, J.; Layton, A. Numerical methods for fluid-structure interaction—A review. *Commun. Comput. Phys.* **2012**, *12*, 337–377. [CrossRef]
143. Davis, M.; Zarnick, E.E. Testing ship models in transient waves. In Proceedings of the 5th Symposium on Naval Hydrodynamics, Bergen, Norway, 10–12 September 1964; Volume 507.
144. Windt, C.; Davidson, J.; Ringwood, J.V. High-fidelity numerical modelling of ocean wave energy systems: A review of computational fluid dynamics-based numerical wave tanks. *Renew. Sustain. Energy Rev.* **2018**, *93*, 610–630. [CrossRef]
145. Windt, C.; Davidson, J.; Schmitt, P.; Ringwood, J.V. On the assessment of numerical wave makers in CFD simulations. *J. Mar. Sci. Eng.* **2019**, *7*, 47. [CrossRef]
146. Jacobsen, N.G. *waves2Foam Manual*; Deltares, The Netherlands, Research Gate: Berlin, Germany, 2017; Volume 570.
147. Alfonsi, G. Reynolds-averaged Navier–Stokes equations for turbulence modeling. In *Applied Mechanics Reviews*; American Society of Mechanical Engineers: New York City, USA, 2009; Volume 62, p. 040802 .
148. Bredberg, J. *On Two-Equation Eddy-Viscosity Models*; Department of Thermo and Fluid Dynamics, Chalmers University of Technology: Göteborg, Sweden, 2001.
149. Menter, F.R. Two-equation eddy-viscosity turbulence models for engineering applications. *AIAA J.* **1994**, *32*, 1598–1605. [CrossRef]
150. Sanderse, B.; Van der Pijl, S.; Koren, B. Review of computational fluid dynamics for wind turbine wake aerodynamics. *Wind Energy* **2011**, *14*, 799–819. [CrossRef]
151. de Oliveira, M.; Puraca, R.; Carmo, B. Blade-resolved numerical simulations of the NREL offshore 5 MW baseline wind turbine in full scale: A study of proper solver configuration and discretization strategies. *Energy* **2022**, *254*, 124368. [CrossRef]
152. Wang, L.; Robertson, A.; Jonkman, J.; Yu, Y.H. Uncertainty assessment of CFD investigation of the nonlinear difference-frequency wave loads on a semisubmersible FOWT platform. *Sustainability* **2020**, *13*, 64. [CrossRef]
153. Popko, W.; Vorpahl, F.; Zuga, A.; Kohlmeier, M.; Jonkman, J.; Robertson, A.; Larsen, T.J.; Yde, A.; Sætertrø, K.; Okstad, K.M.; et al. Offshore code comparison collaboration continuation (OC4), phase 1-results of coupled simulations of an offshore wind turbine with jacket support structure. In Proceedings of the ISOPE International Ocean and Polar Engineering Conference, Rhodes, Greece, 17–22 June 2012; ISOPE: Mountain View, CA, USA, 2012; p. ISOPE–I.
154. Robertson, A.; Jonkman, J.; Musial, W.; Vorpahl, F.; Popko, W. *Offshore Code Comparison Collaboration, Continuation: Phase II Results of a Floating Semisubmersible Wind System*; National Renewable Energy Lab. (NREL): Golden, CO, USA, 2013.
155. Robertson, A.N.; Wendt, F.F.; Jonkman, J.M.; Popko, W.; Vorpahl, F.; Stansberg, C.T.; Bachynski, E.E.; Bayati, I.; Beyer, F.; de Vaal, J.B.; et al. OC5 project phase I: Validation of hydrodynamic loading on a fixed cylinder. In Proceedings of the ISOPE International Ocean and Polar Engineering Conference, Kona, HI, USA, 21–26 June 2015; ISOPE: Mountain View, CA, USA, 2015; p. ISOPE-I-15-116 .
156. Robertson, A.N.; Wendt, F.; Jonkman, J.M.; Popko, W.; Borg, M.; Bredmose, H.; Schlutter, F.; Qvist, J.; Bergua, R.; Harries, R.; et al. OC5 Project Phase Ib: Validation of hydrodynamic loading on a fixed, flexible cylinder for offshore wind applications. *Energy Procedia* **2016**, *94*, 82–101. [CrossRef]
157. Popko, W.; Huhn, M.L.; Robertson, A.N.; Jonkman, J.M.; Wendt, F.; Müller, K.; Kretschmer, M.L.; Vorpahl, F.; Hagen, T.R.; Galinos, C.; et al. Verification of Numerical Offshore Wind Turbine Models Based on Full Scale Alpha Ventus Data within OC5 Phase III. In Proceedings of the ASME 2018 37th International Conference on Ocean, Offshore and Arctic Engineering-Volume 10: Ocean Renewable Energy, Madrid, Spain, 17–22 June 2018.
158. Popko, W.; Robertson, A.; Jonkman, J.; Wendt, F.; Thomas, P.; Müller, K.; Kretschmer, M.; Ruud Hagen, T.; Galinos, C.; Le Dreff, J.B.; et al. Validation of numerical models of the offshore wind turbine from the alpha ventus wind farm against full-scale measurements within OC5 phase III. In Proceedings of the International Conference on Offshore Mechanics and Arctic Engineering, Glasgow, UK, 9–14 June 2019; American Society of Mechanical Engineers: New York City, USA, 2019; Volume 58899, p. V010T09A065.
159. Robertson, A.N.; Gueydon, S.; Bachynski, E.; Wang, L.; Jonkman, J.; Alarcon, D.; Amet, E.; Beardsell, A.; Bonnet, P.; Boudet, B.; et al. OC6 Phase I: Investigating the underprediction of low-frequency hydrodynamic loads and responses of a floating wind turbine. *J. Physics Conf. Ser.* **2020**, *1618-3*, 032033. [CrossRef]
160. Wang, L.; Robertson, A.; Jonkman, J.; Yu, Y.H.; Koop, A.; Borràs Nadal, A.; Li, H.; Bachynski-Polić, E.; Pinguet, R.; Shi, W.; et al. OC6 Phase Ib: Validation of the CFD predictions of difference-frequency wave excitation on a FOWT semisubmersible. *Ocean Eng.* **2021**, *241*, 110026. [CrossRef]
161. Bergua, R.; Robertson, A.; Jonkman, J.; Platt, A.; Page, A.; Qvist, J.; Amet, E.; Cai, Z.; Han, H.; Beardsell, A.; et al. OC6 Phase II: Integration and verification of a new soil–structure interaction model for offshore wind design. *Wind Energy* **2022**, *25*, 793–810. [CrossRef]

162. Cioni, S.; Papi, F.; Pagamonci, L.; Bianchini, A.; Ramos-García, N.; Pirrung, G.; Corniglion, R.; Lovera, A.; Galván, J.; Boisard, R.; et al. On the characteristics of the wake of a wind turbine undergoing large motions caused by a floating structure: An insight based on experiments and multi-fidelity simulations from the OC6 Phase III Project. *Wind Energy Sci. Discuss.* **2023**, *2023*, 1–37. [CrossRef]
163. Bergua, R.; Robertson, A.; Jonkman, J.; Alarcón Fernández, D.; Trubat Casal, P. OC6 project Phase IV: Validation of numerical models for novel floating offshore wind support structures. *Wind Energy Sci.* **2024**, *9*, 1025–1051. [CrossRef]
164. IEA Wind TCP Task 56. OC7 Project (Offshore Code Comparison Collaboration 7). IEA Wind TCP. 2024. Available online: https://iea-wind.org/task-56-oc7-project-offshore-code-comparison-collaboration-7 (accessed on 24 September 2024).
165. Chitteth Ramachandran, R.; Desmond, C.; Judge, F.; Serraris, J.J.; Murphy, J. Floating wind turbines: Marine operations challenges and opportunities. *Wind Energy Sci.* **2022**, *7*, 903–924. [CrossRef]
166. Panchigar, D.; Kar, K.; Shukla, S.; Mathew, R.M.; Chadha, U.; Selvaraj, S.K. Machine learning-based CFD simulations: A review, models, open threats, and future tactics. *Neural Comput. Appl.* **2022**, *34*, 21677–21700. [CrossRef]
167. Kareem, A. Emerging frontiers in wind engineering: Computing, stochastics, machine learning and beyond. *J. Wind Eng. Ind. Aerodyn.* **2020**, *206*, 104320. [CrossRef]
168. Wu, T.; Snaiki, R. Applications of machine learning to wind engineering. *Front. Built Environ.* **2022**, *8*, 811460. [CrossRef]
169. Wang, H.; Cao, Y.; Huang, Z.; Liu, Y.; Hu, P.; Luo, X.; Song, Z.; Zhao, W.; Liu, J.; Sun, J.; et al. Recent Advances on Machine Learning for Computational Fluid Dynamics: A Survey. *arXiv* **2024**, arXiv:2408.12171.
170. Vinuesa, R.; Brunton, S.L. Enhancing computational fluid dynamics with machine learning. *Nat. Comput. Sci.* **2022**, *2*, 358–366. [CrossRef] [PubMed]
171. Masoumi, M. Machine learning solutions for offshore wind farms: A review of applications and impacts. *J. Mar. Sci. Eng.* **2023**, *11*, 1855. [CrossRef]
172. Eivazi, H.; Tahani, M.; Schlatter, P.; Vinuesa, R. Physics-informed neural networks for solving Reynolds-averaged Navier–Stokes equations. *Phys. Fluids* **2022**, *34*, 075117. [CrossRef]
173. Kim, Y.; Choi, Y.; Widemann, D.; Zohdi, T. A fast and accurate physics-informed neural network reduced order model with shallow masked autoencoder. *J. Comput. Phys.* **2022**, *451*, 110841. [CrossRef]
174. Eivazi, H.; Wang, Y.; Vinuesa, R. Physics-informed deep-learning applications to experimental fluid mechanics. *Meas. Sci. Technol.* **2024**, *35*, 075303. [CrossRef]
175. Markidis, S. The old and the new: Can physics-informed deep-learning replace traditional linear solvers? *Front. Big Data* **2021**, *4*, 669097. [CrossRef]
176. Kochkov, D.; Smith, J.A.; Alieva, A.; Wang, Q.; Brenner, M.P.; Hoyer, S. Machine learning–accelerated computational fluid dynamics. *Proc. Natl. Acad. Sci. USA* **2021**, *118*, e2101784118. [CrossRef]
177. Després, B.; Jourdren, H. Machine learning design of volume of fluid schemes for compressible flows. *J. Comput. Phys.* **2020**, *408*, 109275. [CrossRef]
178. Bar-Sinai, Y.; Hoyer, S.; Hickey, J.; Brenner, M.P. Learning data-driven discretizations for partial differential equations. *Proc. Natl. Acad. Sci. USA* **2019**, *116*, 15344–15349. [CrossRef]
179. List, B.; Chen, L.W.; Thuerey, N. Learned turbulence modelling with differentiable fluid solvers: physics-based loss functions and optimisation horizons. *J. Fluid Mech.* **2022**, *949*, A25. [CrossRef]
180. Deshmukh, A.; Allison, J. Simultaneous structural and control system design for horizontal axis wind turbines. In Proceedings of the 54th AIAA/ASME/ASCE/AHS/ASC Structures, Structural Dynamics, and Materials Conference, Boston, MA, USA, 8–11 April 2013; p. 1533.
181. Froese, G.; Ku, S.Y.; Kheirabadi, A.C.; Nagamune, R. Optimal layout design of floating offshore wind farms. *Renew. Energy* **2022**, *190*, 94–102. [CrossRef]
182. Cao, L.; Ge, M.; Gao, X.; Du, B.; Li, B.; Huang, Z.; Liu, Y. Wind farm layout optimization to minimize the wake induced turbulence effect on wind turbines. *Appl. Energy* **2022**, *323*, 119599. [CrossRef]
183. Lozon, E.; Hall, M. Coupled loads analysis of a novel shared-mooring floating wind farm. *Appl. Energy* **2023**, *332*, 120513. [CrossRef]
184. Lopez-Olocco, T.; Liang, G.; Medina-Manuel, A.; Ynocente, L.S.; Jiang, Z.; Souto-Iglesias, A. Experimental comparison of a dual-spar floating wind farm with shared mooring against a single floating wind turbine under wave conditions. *Eng. Struct.* **2023**, *292*, 116475. [CrossRef]
185. Micallef, D.; Rezaeiha, A. Floating offshore wind turbine aerodynamics: Trends and future challenges. *Renew. Sustain. Energy Rev.* **2021**, *152*, 111696. [CrossRef]
186. Liang, Z.; Liu, H. Layout optimization of an offshore floating wind farm deployed with novel multi-turbine platforms with the self-adaptive property. *Ocean Eng.* **2023**, *283*, 115098. [CrossRef]
187. Bashetty, S.; Ozcelik, S. Design and stability analysis of an offshore floating multi-turbine platform. In Proceedings of the 2020 IEEE Green Technologies Conference (GreenTech), Oklahoma City, OK, USA, 1–3 April 2020; IEEE: New York, NY, USA, 2020; pp. 184–189.

188. Fenu, B.; Attanasio, V.; Casalone, P.; Novo, R.; Cervelli, G.; Bonfanti, M.; Sirigu, S.A.; Bracco, G.; Mattiazzo, G. Analysis of a gyroscopic-stabilized floating offshore hybrid wind-wave platform. *J. Mar. Sci. Eng.* **2020**, *8*, 439. [CrossRef]
189. Ding, S.; Yan, S.; Han, D.; Ma, Q. Overview on hybrid wind-wave energy systems. In Proceedings of the 2015 International Conference on Applied Science and Engineering Innovation, Jinan, China, 30–31 August 2015; Atlantis Press: Dordrecht, The Netherlands, 2015; pp. 502–507.